Sea-level rise, localized subsidence, and increased storminess promote saltmarsh transgression across low-gradient upland areas

Carson B. Miller[1], Antonio B. Rodriguez[1*], Molly C. Bost[1]

[1]*Institute of Marine Sciences, University of North Carolina at Chapel Hill, 3431 Arendell St., Morehead City, NC 28557, USA.*

*Corresponding author: Antonio B. Rodriguez, abrodrig@email.unc.edu, 252-726-6841 x-140
3431 Arendell St., Morehead City, NC 28557, USA.

Abstract

Saltmarsh area is decreasing globally from natural and anthropogenic stressors. Accelerating relative sea-level rise (SLR) is projected to exacerbate losses if not offset by upland saltmarsh migration (transgression). In the absence of coastal upland development, saltmarsh transgression rates increase with accelerating SLR and lower upland surface gradients. Storm wind and surge stress coastal upland forests causing defoliation, uprooting, and soil salinization, which makes upland areas more habitable for saltmarsh species and can promote transgression. This study aims to elucidate the contribution of storms to saltmarsh transgression by reconstructing transgression rates over the past 600 years during stormy and non-stormy conditions and fast and slow SLR rates. Our reconstructions are based on the stratigraphic record and historical aerial photography at three sites in North Carolina, U.S.A. where low-gradient pocosin upland grades into expansive saltmarsh. When sea level was rising <0.9 mm yr^{-1}, saltmarsh transgression rates at the two sites where saltmarsh is >100 years were an average of 2 and 10 times faster during a paleo-stormy period (1400-1675 CE) than a subsequent non-stormy period. After 1865 CE when SLR accelerated to 2.4 mm yr^{-1}, transgression rates were an average of 7 times faster than the preceding slow SLR non-stormy period. The two sites where the historical record was not confounded by dredging show transgression was 7 times faster and saltmarsh areas increased an average of 28% during stormy decades than non-stormy decades; however, the rate of transgression only increased at the site with greatest surge during the stormy period characterized by strong northeast winds. Modeled transgression rates, using the paleo-upland slope and a sea level curve, do not match observed transgression rates for the paleo-stormy and rapid SLR periods. Furthermore, the thickness of saltmarsh peat younger than 1957 CE is greater than what would be predicted from independent records of SLR. Changes in the

elevation of the upland surface, which is composed of peat, contributes to the disparity between predicted and observed transgression rates. The upland surface elevation can keep pace with some rates of SLR through vertical accretion; however, salinization and decomposition of upland vegetation from storm surge plus SLR decreases the elevation of the paleo-upland surface and increases accommodation and transgression rates. Along low-gradient coastlines with pocosin upland areas, SLR, subsidence, and storminess are coupled in modulating transgression rates and those processes need to be included in forecasts of saltmarsh response to climate change.

Keywords: saltmarsh, transgression, sea level changes, storminess, Holocene, paleogeography, North America, coastal geomorphology, micropaleontology (foraminifers), radiogenic isotopes

1. Introduction

Many of the ecosystem services saltmarsh provides, including fish and bird habitat (Peterson and Turner, 1994; Van Eerden et al., 2005), water purification (Sousa et al., 2008), carbon sequestration (Mcleod et al., 2011; Theuerkauf et al., 2015), wave attenuation (Barbier et al., 2008; Moller et al., 2014), erosion control (Neumeier and Ciavoloa, 2004; Howes et al., 2010), and tourism/recreation (Altieri et al., 2012; Barbier et al., 2011) scale with area. Saltmarsh area has decreased 25% globally since 1940 CE (Duarte et al., 2008, NOAA Coastal Population Report, 2013) and >50% in many locations such as sites in Australia (Saintilan and Williams, 2000; Rogers et al., 2006), the British Isles (Baily and Pearson, 2007), and New England, USA (Bertness et al., 2002) mainly due to anthropogenic impacts (Kennish, 2001; Bromberg and Bertness, 2005). Saltmarsh restoration, conservation, and management activities are aimed at countering historical and ongoing losses from reclamation, pollution, river impoundments, grazing, and alteration of coastal hydrology (Lotze et al., 2006; Airoldi and Beck, 2007; Gedan et al., 2009); however, many studies conclude that relative sea-level rise (SLR) represents the greatest threat to saltmarsh sustainability (FitzGerald et al., 2008; Crosby et al., 2016). Although SLR is the principal driver of saltmarsh accretion because it creates accommodation (space available for sediments to accumulate in), increases vegetation productivity, and enhances sediment deposition, accelerating SLR can decrease saltmarsh area by shifting the saltmarsh surface into the subtidal realm if rates of saltmarsh vertical accretion lag rates of SLR (Morris et al., 2002; Kirwan and Temmerman, 2009; Kirwan et al., 2010). Historical maps, aerial photography, and satellite imagery show that landward migration of saltmarsh can offset losses (Feagin et al., 2010; Raabe and Stumpf, 2016) and SLR is regarded as the predominant driver (Williams et al., 1999; Kirwan et al., 2016). In some areas, however, landward migration of saltmarsh is not possible due to barriers at the edge of the upland, such as infrastructure or steep topography (Doody, 2013; Torio and Chmura, 2013; Pontee, 2013; Enwright et al., 2016; Thorne et al., 2018).

Fringing saltmarsh forms as SLR inundates upland areas, typically along the protected estuarine shorelines of drowned river valleys, tidal creeks, and barrier islands. Saltmarsh is mainly composed of organic matter from living and decomposing grasses and mineral matter that settles onto the marsh from the water column. The natural conversion of upland landscapes, commonly forest, agricultural fields, and developments, to saltmarsh (saltmarsh transgression) principally occurs due to landward expansion of the intertidal zone (Davis, 1910; Redfield, 1965) and salinization of soils (Bertness, 1988; Thibodeau, 1998). Soil salinization causes an increase in shallow subsidence that can lower surface elevation when the living-root network dies, decays, and compacts, which could promote additional saltmarsh transgression (DeLaune et al., 1994; Brinson et al., 1995; Graham and Mendelssohn, 2014; Stagg et al., 2016; Charles et al., 2019). Saltmarsh transgression is apparent in the geological record (millennial to centennial) from cores that sample saltmarsh peat overlaying older upland soil (Gardner and Porter, 2001; Tornqvist et al., 2004) and in the historical record (decadal) from remote sensing data that resolves the conversion of upland vegetation to saltmarsh vegetation (Raabe and Stumpf, 2016). The rate of saltmarsh transgression is commonly attributed to the surface gradient of the upland and the rate of SLR (Redfield and Rubin, 1962; Redfield, 1965; Oertel and Woo, 1994; Donnelly and Bertness, 2001) with low surface gradients and high rates of SLR promoting rapid saltmarsh transgression (Kirwan et al., 2016; Farron et al., 2020; Langston et al., 2020). Many researchers have exploited the relationship between SLR and saltmarsh transgression to construct Holocene sea-level curves from basal-saltmarsh peat sampled from various elevations (Coleman and Smith, 1964; Gehrels, 1994; Tornqvist et al., 2004; Engelhart and Horton, 2012).

Storm events also facilitate saltmarsh transgression by increasing the amount of light that reaches the understory through physical damage to trees from wind and waves and increasing soil salinity from surge (Brinson et al., 1995; Michener et al., 1997; Cahoon, 2006; Fagherazzi et al., 2019). Some of the physical effects of storm waves on the saltmarsh upland boundary decrease with increasing marsh width and associated damping of wave heights and energy (Shepard et al., 2011; Temmerman et al., 2013; Moller et al., 2014). Salinization of upland soils from storm surge and sea spray has deleterious effects on plants (nonhalophytes; Kozlowski, 1997; Gardner et al., 1991) and can last months in areas that are poorly drained (low surface gradient and low hydraulic conductivity; Blood et al., 1991).

Investigating the response of saltmarsh transgression to an increase in the rate of SLR and storminess is important for developing accurate projections of saltmarsh area under different climate-change scenarios and coastal-development plans. Geological studies identify accelerated saltmarsh transgression during the recent acceleration in SLR at the end of the 19th century and attribute upland surface gradient and rate of SLR as the main determinants of transgression rate (Goodbred et al., 1998; Donnelly and Bertness, 2001; Schieder and Kirwan, 2019). This study builds on that previous work by examining the impact of changes in storminess on the rate of saltmarsh transgression focusing on low-gradient coastal plain areas where saltmarsh upland expansion is projected to have the largest impact on offsetting losses (Kirwan et al., 2016).

Records of saltmarsh transgression during the late Holocene are preserved in the sediments below the existing fringing saltmarsh (Fig. 1a). Given a constant seaward-dipping upland topography, saltmarsh transgression rates are predicted to increase proportionately with the rate of SLR as the intertidal zone moves progressively landward (Fig. 1). Based on the simple conceptual model shown in Figure 1a, we hypothesize that during stormy periods observed rates of saltmarsh transgression, measured directly from the sedimentary record, will increase disproportionately above predicted rates and/or above rates during non-stormy conditions under both slow and rapid SLR (Fig. 1). Alternatively, observed transgression rates will not correspond with predicted values (Fagherazzi et al., 2019), because of upland soil accretion (landward) and subsidence during salinization at the upland-saltmarsh transition zone. To test the hypothesis, we developed records of saltmarsh transgression at three low-gradient sites (gradient <0.001; Figs. 1 and 2). The records include relatively stormy and non-stormy periods that coincided with both slow and rapid rates of SLR.

2. Regional setting

North Carolina, U.S.A. has vast expanses of fringing saltmarsh up to 7 km wide and is ranked 7th in the US for most saltmarsh area (CEC, 2016). The largest area of fringing saltmarsh in North Carolina is located north of Cape Lookout (Fig. 2) where the lower coastal plain is nearly flat, as shown by the 1.5 m elevation contour line positioned (on average) 1.1 km from the estuarine shoreline (Moorhead and Brinson, 1995). These expansive saltmarshes are mostly high marsh, dominated by *Juncus romarianus*, with a narrow band (<5 m wide) of *Spartina alterniflora* at the estuarine shoreline (Brinson, 1991). The upland is mainly a palustrine wetland with poor drainage, dominated by evergreens, and called a pocosin (Brinson, 1991). Pocosin wetlands form thick histosols and are influenced by SLR along their seaward margin, forming a transition zone between the upland and saltmarsh composed of high marsh, a relict forest composed of dead or dying trees called a ghost forest, and shrubs (Brinson, 1991).

The Outer Banks barrier island chain isolates Pamlico Sound and surrounding estuaries from tidal exchange (Luettich et al., 2002). Wind stress and the generation of seiches primarily cause the semi-diurnal variations in estuarine water level observed north of Cape Lookout (Luettich et al., 2002). Winds from the NE excite seich events and push water from north Pamlico Sound into the Neuse River Estuary and Long Bay increasing water levels in southern areas (Giese et al., 1985; Luettich et al., 2002; Reynolds--Fleming and Luettich, 2004; Reed et al., 2008). Meteorological forcing accounted for 77% of the water-level variance in southern Pamlico Sound, based on data collected over an 18-month period, and northerly winds flooded saltmarsh for weeks at a time (Voss et al., 2013). The tides in Core Sound are primarily astronomically driven with an average range of 0.3 m, but water levels are also influenced by its connection with Pamlico Sound to the north and increase with northerly wind directions.

3. Material and methods

3.1 Site Selection and Sampling

The study area of central eastern North Carolina is an excellent site because it is proximal to a high-resolution sea-level curve (<10 cm vertical precision; Kemp et al., 2017) and a paleo-storm record (Mallinson et al., 2011; Fig. 2). The Kemp et al. (2017) sea-level curve extends 2,000 years, is based on foraminiferal assemblages analyzed at 1-cm intervals in saltmarsh strata, and a high-resolution age-depth model based on multiple dating methods (Kemp et al., 2009b). Sea level was rising at a consistently low rate of 0.9 mm yr^{-1} from ~ 0 CE to ~ 1800 CE, after which the rate of SLR accelerated to 2.4 mm yr^{-1} by the end of the 19th century. These are relative rates of SLR that include a model-estimated 0.93 mm yr^{-1} contribution from glacio-isostatic adjustment (Kemp et al., 2017). Between 1400-1675 CE, when the rate of SLR was slow, Mallinson et al. (2011) documented an increase in the number of inlets through the Outer Banks, NC, attributing an increase in nor'easter activity and associated beach erosion, surge, and overwash as the cause (Mallinson et al., 2011). The increase in the cumulative number of inlets that formed over time was used as a proxy for increased storminess in NC and that paleo-stormy period was also recognized across the entire western North Atlantic from event deposits sampled in MA (two sites) and The Bahamas (Donnelly et al., 2015). The changes in SLR and storminess affecting eastern North Carolina since 1300 CE allow us to compare records of saltmarsh transgression during three distinct periods: 1400-1675 CE—a period of increased storminess with slow SLR (0.9 mm yr^{-1}; paleo-stormy period), 1675-1865 CE—a non-stormy period when SLR remained slow (paleo-quiescent period), and 1865 CE-present—a period of rapid SLR (2.4 mm yr^{-1}; rapid SLR period; Kemp et al., 2011).

Saltmarshes generally accrete vertically at the rate of relative SLR and decrease in thickness landward. Based on the Kemp et al. (2017) sea-level curve, a saltmarsh thickness of at least 0.75 m at the estuarine boundary is required for a site to contain a record of saltmarsh transgression that extends back to 1300 CE, the time frame of interest for this study. Peat thickness was initially surveyed at the shoreline of prospective sites using a Russian peat auger, which allowed us to assess the general stratigraphy in the field. Based on peat thickness, we chose three fringing saltmarsh sites to develop records of transgression, including: 1. Jones Bay (JB), a 192-m wide south-facing saltmarsh; 2. Long Bay (LB), an 800-m wide north-facing saltmarsh; and 3. Nelson Bay (NB), a 210-m wide east-facing saltmarsh (Fig. 2). We collected a transect of vibracores and elevation measurements oriented perpendicular from the trend of the upland-saltmarsh boundary. Our aim was to decrease the spacing between cores in areas thought to record saltmarsh response to the paleo-stormy period; however, given difficulty with identifying the base of saltmarsh strata in the field, the goal was never achieved. The cores were collected in 7.6-cm diameter aluminum irrigation pipe, were an average of 3-m long, and sampled the entire thickness of wetland sediment. GPS locations and elevations were collected for each core and between cores using a Trimble R8 RTK-GPS with an average vertical error of ± 3 cm (Supplementary Table 1). Saltmarsh surface-elevation measurements enabled us to relate stratigraphic units and bounding surfaces identified in the cores to the Kemp et al. (2017) sea-level curve. We created stratigraphic cross sections from the 8 or 9 cores collected at each site from the saltmarsh shoreline to the upland-saltmarsh boundary, using the saltmarsh-surface elevation profile as a base from which to hang the cores.

3.2 Sample processing

We split the cores along their long axis and photographed, described, and sampled the cores for foraminifera, to help interpret the stratigraphic units, and stems or leaves for radiocarbon dating. Foraminifera assemblages are commonly used to identify tidal-elevation zones in saltmarsh strata and the supratidal upland environment lacks foraminifera (Culver and Horton, 2005; Horton and Culver, 2008; Kemp et al., 2009a). Sample volumes for foraminiferal analysis were consistently 4 cm^3, taken at 1-cm intervals, and all samples were collected from the center of the core to avoid contamination associated with displacing material around the sides of the core barrel. The sample was washed with deionized water through a 2 mm sieve to collect large organic matter and a 63 µm sieve to collect foraminifera. Samples were inspected wet under a microscope.

Of the 25 total cores, we sampled 18 for radiocarbon dating, 6 from Jones Bay, 8 from Long Bay, and 4 from Nelson Bay. We extracted 8 cm^3 of sediment (sample dimensions were 2 x 2 x 2 cm) from the base of the saltmarsh unit to identify *in-situ* marsh stems or marsh leaves for radiocarbon dating. To avoid vertical roots or stems that would return an anomalously young date, we did not select stems or leaves for dating that were cut during sample extraction to a 2-cm length. Samples were sent to the National Ocean Sciences Accelerator Mass Spectrometry Facility at the Woods Hole Oceanographic Institution for radiocarbon dating and results were calibrated to calendar years using CALIB 7.1 and CALIBomb (Stuiver and Reimer, 1993; Reimer et al., 2013). Calibrated dates (2 SD) commonly include multiple distinct time ranges of variable probability and we generally chose the date range with the highest certainty (Supplementary Table 2). We chose CALIB 7.1 dates outside the most certain range only when stratigraphic position indicated another age range was more appropriate. For the historical part of the record, we compared the post-bomb calibrated radiocarbon dates with the acquisition dates of the aerial photos and chose the age range that included the first documented saltmarsh at the core location (Table 1). The elevations of radiocarbon dated samples were converted to Mean Tide Level (MTL) using Vdatum (Hess et al., 2005). Average saltmarsh vertical accretion rates were calculated by dividing the thickness of the saltmarsh unit by age, which is the difference between the core collection date and the age of the basal-saltmarsh peat, with uncertainty based on the calibrated radiocarbon date range.

3.3 Remote sensing and historical storm record

Modern upland slopes were measured using LiDAR data acquired in 2014 and downloaded from NOAA's Digital Coast Data Access Viewer (https://coast.noaa.gov/dataviewer/#/). Point clouds were manually filtered to remove vegetation and extraneous points using Merrick Advanced Remote Sensing Software 2018, verified by ground measurements obtained using the Trimble R8 RTK-GPS around the edge of the upland, and exported to Surfer 15 (Golden Software, Inc.) to create digital elevation models (DEMs) using a 0.5 m grid cell spacing. Elevation profiles were extracted from the DEMs along a transect at each site extending from the shoreline, through the core locations, and 300 m into the upland forest. Upland slope is the slope of the regression line fit through the profile extending from the edge of the saltmarsh-forest boundary into the upland ± the 95% confidence interval.

To assess historical changes in saltmarsh area, we analyzed aerial photography at the study sites obtained from the USGS Earth Explorer (https://earthexplorer.usgs.gov/) dating back to 1957 CE, the first available image for all sites. We assessed changes to saltmarsh area for each time step, as opposed to displacement of the saltmarsh-upland boundary to avoid large georeferencing error >10 m for some images. The landward edge of the saltmarsh, surveyed in the field, was designated as the boundary between saltmarsh and the upland transition zone, consisting of ghost forest and less salt-tolerant plants (Red Maple, *Acer rubrum*; Magnolia, *Magnolia grandiflora*; and Sweet Pecan, *Carya illinoensis*; Stanturf et al., 2007). Uncertainty was assessed using the sum of squares of the image-resolution and digitizing error. The image-resolution error was calculated by multiplying the perimeter of the digitized marsh area (m) by the cell size. Digitizing error was assessed by having three individuals digitize the same marsh area 3 times using at least four images with differing cell sizes and calculated as the average difference between areas. To compare historical changes in marsh area with storminess, we queried the NOAA Historical Hurricane Track database (https://oceanservice.noaa.gov/news/historical-hurricanes/) for storms since 1955 CE with sustained wind speeds >55.5 km hr^{-1} and centers that passed within a 75-km radius around a coordinate central to the sites (18S 370276.77 m E 3863983.09 m N). We categorized the output into three bins including: 1. the total number of events, 2. major hurricanes (category 3 or greater), and 3. NE wind events.

3.4 Calculating and modeling transgression rates

The contact between saltmarsh and upland sedimentary units, sampled in each core, represents the paleo-upland surface. This flooding surface should decrease in age landward with decreasing depth. Transgression rates were measured between adjacent cores using the following equation: $(x_i - x_{i-1}) / (t_i - t_{i-1})$, where x_i is the position of the core along the transect and t_i is the calibrated radiocarbon age of the basal saltmarsh sample. Uncertainty in transgression rate is based on the longest and shortest time range between the dated samples. To compare saltmarsh transgression rates measured during a stormy period with transgression rates measured during a non-stormy period, ideally, we would have two adjacent cores with basal saltmarsh-peat date ranges that do not overlap and fall entirely within each period. That ideal was not always achieved, and in places, we had to measure transgression rates across the boundary between stormy and non-stormy periods. We designated the measured transgression rate as representing a stormy or non-stormy period based on the period that overlapped the most with the time frame from which transgression was measured.

Assuming SLR is the principal driver of saltmarsh landward migration across upland topography, we modeled transgression rates over the last 600 years using the Kemp et al. (2017) relative sea-level curve and the paleo-upland slope. Paleo-upland slopes were calculated between cores by using the slope equation $(y_i - y_{i-1})/(x_i - x_{i-1})$, where y_i is the elevation of the contact between upland peat and saltmarsh strata and x_i is the position of the core along the transect. We sampled the Kemp et al. (2017) relative sea-level curve over the same time periods for which we measured transgression rates (t_i-t_{i-1}) and calculated an average rate of SLR by linear regression. The modeled or predicted transgression rate is the rate of SLR during the period, divided by the paleo-upland slope. Uncertainty for modeled transgression was assessed using only the 95% confidence interval for the sea-level regression line because the small elevation and distance errors have negligible effects on paleo-upland slope.

4. Results and interpretation

4.1 Stratigraphy

Cores obtained from each site sampled a basal clay unit overlain by peat (Fig. 3). The upper part of the clay unit is commonly variegated grey (5YR 6/1) and yellow (10YR 7/6) with roots, wood, and large (up to 5-cm diameter) burrows and the unit was undifferentiated. The variegated color is evidence of oxidation attributed to subaerial exposure and we interpret this unit was deposited during the Pleistocene. The contact between the Pleistocene clay and the peat unit was generally sharp and consisted of dark reddish brown (5YR 2.5/2), silty organic material, visible *S. alterniflora* and *J. romarianus* roots and stems near the top, as well as wood fragments. Degradation of plant material increases down core and the color of the peat becomes darker (5YR 2.5/1). *S. alterniflora* plant material was only found at the top of the cores close to the shoreline where live *S. alterniflora* was at the surface.

The peat could not be differentiated into upland and saltmarsh units based on texture, composition, and/or color; however, those two units should be present because saltmarsh colonizes the upland as the intertidal zone extends landward through time (Fig. 3). The peat does not consistently decrease thickness towards the upland boundary providing additional evidence that two stacked peat units exist at the sites. The most landward core at each site, obtained from the edge of the upland, sampled 1.5-0.5 m of peat (Fig. 3). In this low-gradient setting, saltmarsh could not have formed peat 1.5-0.5 m thick at the edge of the upland because this should be the youngest part of the saltmarsh and even a 0.5-m thick saltmarsh peat would have taken about 150 years to form assuming vertical accretion is directly related to the rate of SLR (~2.4 mm yr^{-1}). Using the initial presence of foraminifera in the peat to differentiate between upland and saltmarsh units results in a saltmarsh peat that becomes thinner in a landward direction with thicknesses ranging between 101-27 cm at Jones Bay, 83-31 cm at Long Bay, and 51-21 cm at Nelson Bay (Fig. 3).

The stratigraphy of our sites is like what Kemp et al. (2011) identified at Tump Point using similar methods, including Pleistocene clay overlain by thick peat composed of lower freshwater and upper saltmarsh units. It is difficult to compare our results with other previous studies conducted in the area because different criteria were used to identify the base of saltmarsh peat. Young (1995) recognized a similar stratigraphy in cores collected near our Long Bay Site, but at a location where saltmarsh formed above an old Carolina Bay (Prouty, 1952). That study did not include site or core coordinates, determined the base of the saltmarsh peat visually and on an increase in bulk density with depth, and presents saltmarsh elevations that are >0.75 cm too high (~1.0 m relative to mean high water; Young, 1995). The contact between the Pleistocene clay and upland peat is a disconformity and that interface was visually interpreted as the base of saltmarsh near the Long Bay Site by Schieder and Kirwan (2019). The contact between upland and saltmarsh peat (paleo-upland surface) is interpreted here based on micropaleontological indicators to be above that disconformity, is a time-transgressive flooding surface, and the average paleo-upland slopes, are 0.0038 ± 0.002 for Jones Bay, 0.0021 ± 0.0008 for Long Bay, and 0.003 ± 0.0006 for Nelson Bay. Those slopes are steeper than the average modern upland slopes of 0.0007 ± 0.0001 for Jones Bay, 0.0011 ± 0.0002 for Long Bay, and $0.0013 \pm 8.5 \times 10^{-5}$ for Nelson Bay.

4.2 Chronology

The records of saltmarsh transgression at the sites span different periods of time. This occurred because we could not visually differentiate between upland and saltmarsh peat in the field and although all sites had >0.75 m of peat at the shoreline, only the top of the unit is saltmarsh. The oldest median radiocarbon dates from basal saltmarsh peat samples at each site are 1514 CE for Jones Bay, 1315 CE for Long Bay, and 1957 CE for Nelson Bay (Table 1). Variability in the duration of the saltmarsh peat record among sites is mainly controlled by the elevation of the top of the Pleistocene clay unit. The contact between Pleistocene clay and peat is highest at the Nelson Bay Site where we have the shortest and most recent record of saltmarsh transgression (Fig. 3). Radiocarbon dates of basal-saltmarsh peat for each transect generally become younger in a landward direction. The date of basal-saltmarsh peat sampled in Jones Bay core 5 is 11-84 years younger than the date sampled in the adjacent landward core 6 (using the 1650-1673 CE date range for Core 5 as opposed to the median probability date of 1784 CE); therefore, the core 5 date excluded from the study (Table 1). In Nelson Bay, the radiocarbon date of basal-saltmarsh peat in core 8 is 40 years younger than the date sampled in the adjacent more landward core 3b and was also excluded from the study (Table 1). In addition, aerial photos that show saltmarsh at the location of core 8 before 1999 CE confirm that the date is anomalously young. The date and depth of the basal-saltmarsh peat, which is composed of *J. romarianus* (high marsh), should plot close to the Kemp et al. (2017) sea-level curve because SLR is a dominant driver of saltmarsh transgression (Fig. 4a). Most radiocarbon date ranges fall within the uncertainty band around the Kemp et al. (2017) sea level curve with outliers < 0.11 m from the 95% uncertainty band (Fig. 4a).

Saltmarsh average vertical accretion rates vary within and among sites, range from 1.2 to 8.3 mm yr^{-1}, and are ≥ the average rate of SLR (within error) derived from the Kemp et al. (2017) sea-level curve (Fig. 4b). Average vertical accretion rates at Jones and Long bays are lowest at the shoreline and increase toward the upland boundary as the saltmarsh becomes younger; however, average vertical accretion rates at Nelson Bay, which formed since 1957 CE, is higher at the shoreline and decreases landward. Saltmarsh that colonized the area prior to 1892 CE show vertical accretion rates that generally match the average rate of SLR. Vertical saltmarsh accretion rates of 6.0 mm yr^{-1} for Jones Bay, 5.0 mm yr^{-1} for Long Bay and 3.8, 5.5 and 8.4 mm yr^{-1} for Nelson Bay, all from locations where saltmarsh colonized the upland after 1892 CE, exceed the ~2.4 ± 0.7 mm yr^{-1} rate of local SLR (Fig. 4b; Kemp et al., 2017).

4.3 Transgression rates

Saltmarsh transgression rates vary through time from 0.17 to 15.03 m yr^{-1} (median rates). During the paleo-stormy period from 1400 to 1675 CE when the average rate of SLR was ~0.9 mm yr^{-1}, Jones Bay and Long Bay had median transgression rates of 1.75 m yr^{-1} and 0.33 m yr^{-1}, respectively (Fig. 5). At Jones Bay, the maximum transgression rate plotted for the paleo-stormy period is an underestimate because the age ranges of basal saltmarsh peat in cores 1 (1514-1600 CE) and 6 (1463-1639 CE) overlap (Fig. 3; Table 1). That transgression rate is within the resolution of the radiocarbon method and minimum and maximum transgression rates are based on the periods 1514-1639 CE and 1600-1639 CE, respectively, which excludes the older 1463-1600 CE part of the date range for core 6. At Long Bay, transgression rate during the paleo-stormy period is also a minimum because the time over which transgression rates were measured incorporate some of the earlier pre-1400 CE non-stormy period (Fig. 5). During the subsequent paleo-quiescent period, sea level was still rising at that same slow rate (Kemp et al., 2017), but median transgression rates decreased to 0.18 m yr^{-1} at Jones Bay and 0.17 m yr^{-1} at Long Bay. When taking error into account, even the lowest possible transgression rates during the stormy period at Jones and Long bays exceed the highest possible transgression rates during the non-stormy period.

When the rate of SLR accelerated to 2.4 mm yr^{-1} at the end of the 19th century, the average of the median transgression rates at Long Bay (n=3) increased to 1.16 m yr^{-1} over the period from ~1808 CE to present. At the beginning of the rapid SLR period the saltmarsh transgression rate at Long Bay is within the resolution of the radiocarbon dating method and the actual maximum saltmarsh transgression rate could be much greater than what is plotted (Fig. 5). The date ranges of the basal saltmarsh peat in Long Bay cores 7 (1808-1892 CE) and 8 (1867-1918 CE) overlap and the maximum transgression rate is based on the period 1892-1918 (Fig. 3, Table 1). At Jones Bay, no increase in transgression rate was observed over the period 1782-1972 CE, but half of that period incorporates the earlier paleo-quiescent period when sea level was rising slower. In addition, a ditch was excavated, and dredge spoil was deposited along its banks at the Jones Bay saltmarsh-upland boundary sometime between 1957 and 1961 CE. This anthropogenic increase in elevation disturbed the recent part of the saltmarsh-transgression record at the Jones Bay Site. At Nelson Bay, where the record of saltmarsh transgression is limited to the last 60 years, the median rate of transgression was 8.63 m yr^{-1} (n=2). The periods over which transgression rates are measured during the rapid SLR period are an order of magnitude shorter than the paleo-stormy and paleo-quiescent periods.

4.4 Historical changes in saltmarsh area and storminess

Historical aerial photography from Long and Nelson bays, analyzed from 1957-2018 CE, shows that saltmarsh area increased discontinuously (Fig. 6). We assume that most of the measured increases in saltmarsh area were due to conversion of upland forest to saltmarsh, as opposed to expansion of the saltmarsh into the estuary because increases in saltmarsh area were associated with a landward shift in the upland boundary that exceeded the georeferencing error, the shape of the crenulated shoreline remained constant through time, and the images that cover the last 50 years of the record with georeferencing errors <1 m show a static shoreline position (< georeferencing error). Aerial photography from Jones Bay was not used in this analysis because of the excavation of the ditch at the upland-saltmarsh boundary that prevented transgression. The storm record from 1955-2018 CE shows variability in storminess (Fig. 6). The largest storm to impact the area was in 1958 CE when the eye of Hurricane Helene (category 4) passed offshore of the sites. Saltmarsh areas at Long and Nelson bays increased 512,607 m^2 and 158,490 m^2, respectively, after Hurricane Helene during the period 1957-1970 CE. In addition to Hurricane Helene, the period 1954-1960 includes four of the ten highest water levels ever recorded at the nearby NOAA long-term Beaufort gauge (8656483) located 30 km southwest of the Nelson Bay Site (Sept. 12, 1960; Fig. 6). The average frequency of all storm events from 1950 to 2000 is 5.2 ± 1.3 storms $decade^{-1}$ (± 1 SD; min=4; max=7) and increased to 10 and 8 storms $decade^{-1}$ during the 2000s and 2010s, respectively. The increase in storminess since 2000 CE was mainly driven by events associated with strong winds from the northeast that promote sustained flooding of areas around Long Bay (Giese et al., 1985; Voss et al., 2013). There was no change in saltmarsh area (within measurement error) at both sites from 1970 to 1999 CE; however, during the period

1999 to 2018 CE the saltmarsh area at Long Bay increased 425,401 m^2 and remained constant at Nelson Bay (within measurement error).

4.5 Modeled transgression rates

Observed and modeled transgression rates are compared to test whether our measurements can be explained solely by upland slope and SLR (Kirwan et al., 2016; Pethick, 2001; Doyle et al., 2010; Fig. 7). The paleo-slope of the upland is negative (slopes landward) in some places along the Jones and Long bays cross sections, which would preclude modeling saltmarsh transgression rates. At Long Bay, the landward sloping upland is distal to where we have radiocarbon dates and is outside the timeframe of this study. At Jones Bay, transgression rates were modeled using the paleo-upland slope measured between cores 1 and 6, ignoring the landward-sloping distal area between cores 1 and 5 because of the anomalously young radiocarbon date measured in core 5 (Fig. 3). The low transgression rates (<0.30 m yr^{-1}) measured during the paleo-quiescent period fall on the 1:1 line (Fig. 7). In addition, the transgression rate measured at Jones Bay over the period 1782-1972 CE is close to the 1:1 line; however, that date range (black point; Fig. 7) was difficult to classify because it is split between the paleo-quiescent period and the rapid SLR period and transgression rates are confounded by dredge-spoil disposal at the upland boundary. Observed transgression since 1850 CE was > modeled for most of the measurements, with the exception being Long Bay (1905-1957 CE). For that point, rates were measured between cores 8 and 9 where the paleo-upland slope is zero (Fig. 3) and the model output shows instantaneous transgression (magenta point; Fig. 7). Observed transgression measured during the paleo-stormy period plot ≤ to modeled values; however, measured transgression rates for both of those points are minimum values (red points; Fig. 7).

The dates used for Jones Bay (1514-1639 CE) have overlapping ranges, which suggest observed transgression rates are likely much higher than what can be measured. The observed transgression rate at Long Bay (1335-1598 CE) is also a minimum because the calculation includes ~50 years of non-stormy conditions prior to 1400 CE.

5. Discussion

5.1 Storminess and rate of sea-level rise

The paleo-stormy period (1400-1675 CE) was recognized by Donnelly et al., (2015) as extending along the entire western North Atlantic region, suggesting that the increase in saltmarsh transgression rates at Jones and Long bays, >10 and 2 times higher than the subsequent paleo-quiescent period, respectively, was more widespread. In addition to frequent storm surge, the sites experienced a higher astronomical tidal range during the paleo-stormy period, a result of more inlets along the Outer Banks that increased connectivity between Pamlico Sound and the open ocean (Mallinson et al., 2011; Mulligan et al., 2019). The increase in storminess and higher astronomical tidal range, which could have been as much as 5 cm higher than present on average (Mulligan et al., 2019), extended inundation of the upland landward, driving the high rates of saltmarsh transgression observed at Jones and Long bays. As conditions became less stormy, the Outer Banks became more continuous, the astronomical tidal range decreased, and saltmarsh transgression rates decreased in response. Saltmarsh transgression rates at Jones and Long bays during the paleo-quiescent period when SLR was 0.9 mm yr^{-1} (1675-1865 CE) were 0.17-0.18 m yr^{-1}, lower than the long-term average from ~800 CE to1872 CE that Schieder and Kirwan (2019) reported (0.32 m yr^{-1}) from a nearby site, which included the paleo-stormy period.

Transgression rates at our sites during the rapid SLR period (0.75-2.2 m yr^{-1}; 1865 CE-present) are similar to rates observed across other low-gradient upland areas in Florida (2.3 m yr^{-1}), North Carolina (1.65-4.61 m yr^{-1}), Virginia (3.3 m yr^{-1}), and Maryland (1.87-2.18 m yr^{-1}; Raabe and Stumpf, 2016; Schieder and Kirwan, 2019). Sea level was rising 2.7 times faster and the rate of saltmarsh transgression at Long Bay was 7 times higher during the rapid SLR period than the previous paleo-quiescent period. The increased rate of saltmarsh transgression, excluding stormy decades post-1950 CE, was proportionate to the increase during the paleo stormy period. This suggests that at the centennial time scale, an increase in storminess can be as effective as an increase in SLR at accelerating saltmarsh transgression across low-gradient upland areas. Like SLR, increased storminess at our sites caused elevated estuarine water level from surge and a higher astronomical tidal range from the additional inlets that increased exchange between the coastal ocean and Pamlico Sound (Mallinson et al., 2011; Mulligan et al., 2019).

Only the historical record of saltmarsh transgression was preserved in the sediments at the Nelson Bay Site and the high-temporal resolution record allowed us to measure transgression rates from both the core transect and aerial photography. Around the time category 4 Hurricane Helene (1958 CE) passed by the Nelson Bay Site, saltmarsh area increased 36% from 1957 to 1970 CE. Hurricane Helene was the largest storm on record to impact the area and was preceded and followed by multiple extreme high-water events. The most rapid saltmarsh transgression rate of our study (13.7-16.6 m yr^{-1}) was recorded between 1957 and 1962 CE by cores 1 to 3b obtained from that newly formed saltmarsh (Fig. 3). Over the next 50 years the Nelson Bay saltmarsh area did not increase above measurement error despite continuously high rates of SLR. Saltmarsh transgression in Long Bay responded similarly to Hurricane Helene and the high-water events, increasing in area 30% from 1957 to 1970 CE, followed by a subsequent 30-year period of no measurable areal increase. Rapid transgression from 1957-1970 followed by decades of no transgression, suggests that major pulses of high-water can drive the saltmarsh landward discontinuously. Transgression rates measured during periods of numerous extreme high-water events exceed what would be predicted only from SLR.

From 1999-2018 CE, saltmarsh area at Long Bay increased 19% unlike Nelson Bay that showed no increase in area during those two decades. More than half of the storms after 1999 CE (67%) were associated with northeasterly winds and 5 of the 6 hurricanes (category 1 and 2) that impacted the sites during those two decades had the strongest winds from the northeast. The increase in saltmarsh area post 1999 CE at Long Bay was due to the northeast-facing orientation of its saltmarsh shoreline and upland boundary, where fetch is greatest for storms with northeasterly winds that increase water-levels in southwestern areas of Pamlico Sound (Reynolds--Fleming and Luettich, 2004; Reed et al., 2008). Christian et al. (1990) showed that these saltmarshes and uplands are commonly flooded >1 m deep during NE-wind events, which can last for over a week. The Nelson Bay Site is less influenced by persistently high-water level during northeast winds because Nelson Bay is positioned along the western shoreline of Core Sound and has greater connectivity with the open ocean through Barden Inlet to the south and Drum Inlet located almost directly across the Sound, 6 km away (Figs. 2 and 6). Those disparate transgression rates post 1999 CE at Nelson and Jones bays illustrate that storm characteristics, such as wind direction and track, are important drivers of transgression rate, in addition to SLR and changes in storm frequency and magnitude. Leonardi et al. (2016) demonstrated that smaller, more frequent storms with recurrence intervals of ~2-3 months cause more saltmarsh shoreline erosion than larger storms, like hurricanes; however, the aerial imagery analysis from the sites presented here show that both major hurricanes and smaller more frequent events, such as nor'easters, can produce large landward shifts in saltmarsh area not associated with significant shoreline erosion. At our sites, those storms caused water levels to exceed the marsh platform elevation and high water likely protected the shoreline from wave attack (Everett et al., 2019).

5.2 Vertical accretion rates and localized subsidence

The occurrence of saltmarsh transgression in response to SLR also depends on the vertical accretion rate of upland soil. If the upland gains elevation through vertical accretion at a rate matching relative SLR, then saltmarsh transgression should be limited. Pocosin soils in coastal North Carolina and Virginia (Brinson et al. 1991) show vertical accretion rates of 0.15-0.56 cm yr^{-1}, generally keeping pace with pre-1865 CE and historical rates of SLR (Drexler et al., 2017; McTigue et al., 2019). Despite upland elevation having the potential to increase with SLR, our stratigraphic data show continuous transgression at the sites, albeit at varying rates. Storm-related stresses to upland vegetation and soils are required for saltmarsh transgression of low gradient pocosin wetlands that vertically accrete with SLR.

The cores obtained close to the upland boundary suggest that high sediment accommodation in areas recently colonized by saltmarsh is an important driver for transgression. Vertical accretion rates extrapolated from the basal saltmarsh peat younger than 1950 CE to the surface exceed the rate of local SLR ($\sim 2.4 \pm 0.7$ mm yr^{-1}; Kemp et al., 2017; Fig. 4b). While rates of saltmarsh vertical accretion $\geq$ SLR is commonly observed along saltmarsh shorelines and on saltmarsh platforms (Morris et al., 2002; Chmura and Hung, 2004; Ouyang and Lee, 2014; Gonneea et al., 2019), at the upland boundary saltmarsh accommodation is limited due to upland elevations that gradually increase landward and accretion rates should be driven by SLR

(Bricker-Urso et al., 1989). The high rates of saltmarsh accretion near the upland boundary at the sites are likely due to local subsurface processes increasing sediment accommodation in excess of regional SLR from the decomposition and compaction of freshwater wetland soils following plant mortality and salinization (DeLaune et al., 1994; Graham and Mendelssohn, 2014; Herbert et al., 2015; Stagg et al., 2016; Charles et al., 2019). Erosion at the upland forest boundary is another factor that could decrease surface elevation, but that is only possible if the saltmarsh fronting the forest was narrow and provided minimal wave damping (Fagherazzi et al., 2019; Moller et al., 2014).

A decrease in the elevation of the paleo-upland surface from decomposition and compaction of upland soil at the sites is supported by projecting the modern upland gradient seaward through the cross sections (projected upland surface), assuming the projected upland surface is analogous to the uncompacted paleo-upland surface for the relatively short period since 1950 CE (Fig. 8). The projected upland surface is above the elevation of the paleo-upland surface across the entire extent of all transects suggesting subsurface processes modified the elevation of the paleo-upland surface. Some of the elevation difference between the surfaces can be explained by natural spatial variations; however, the modern upland surface shows little variation in slope over a 300-m distance (Fig. 2). Furthermore, the elevation offset increases towards the estuarine shoreline with increasing age of the basal-saltmarsh peat. We estimated elevation loss of the paleo-upland surface for the post-1950 CE part of the saltmarsh transgression record, including the most landward cores at Jones and Long bays and the entire core transect at Nelson Bay (Fig. 8). Elevation loss is the elevation of the paleo-upland surface - the elevation of the projected upland surface and decreases landward ranging from 15.7 to 37.4 cm with an average loss of 29.6 cm. Dividing elevation loss by the age of the saltmarsh (the core collection date, 2018 or 2019, minus the date of the basal-saltmarsh peat) suggest average shallow subsidence rates generally decrease as the age of the saltmarsh increases from -19.6 mm yr^{-1} for the last 8 years to -3.7 mm yr^{-1} for the last 61 years. A prominent break in slope exists between the modern upland surface and the subsiding paleo-upland surface around the limit of storm inundation (Fig. 8). This was observed near the upland boundary where the paleo-upland surface has the higher slope, a result of increasing net subsidence away from the upland forest. The core transect at Long Bay does not show this as well as the other two sites because the location of the most landward core is 120 m from the upland boundary.

Shallow subsidence around the edge of the upland explains the thick rapidly accreting saltmarsh sampled near the upland boundary, saltmarsh transgression in areas where upland soils accumulate rapidly, and why predicted rates of saltmarsh transgression based on the slope of the paleo-upland surface and SLR do not match field measurements. These estimates of elevation loss are comparable to values reported by Cahoon et al. (2006) for mangroves (7-11 mm yr^{-1}) up to 8 years after a storm and by Charles et al. (2019) for experiments that manipulated salinization of freshwater wetland soils from the Everglades of Florida (27.5 mm yr^{-1}) after 1 year. Saltmarsh transgression of Pleistocene upland sand and clay is also common (Davis, 1910; Johnson, 1919) but would not be associated with a commensurate elevation loss that requires saltmarsh colonization of hydric upland soil.

5.3 Saltmarsh transgression of low-gradient upland areas

Discontinuous saltmarsh transgression rates documented at the sites supports the ecological ratchet model as conceptualized by Fagherazzi et al. (2019). That model recognizes a landward regeneration upland zone, where both mature trees and seedlings can thrive and a persistence upland zone positioned closer to the saltmarsh, where mature trees survive but SLR prevents seedlings from establishing (Fig. 9). The movement of the saltmarsh-upland forest boundary landward initiates when storm wind and surge cause tree mortality in the persistence zone (Brinson et al., 1995; Michener et al., 1997; Cahoon, 2006). Storms remove upland vegetation making conditions more conducive for saltmarsh colonization, but SLR is necessary to reduce the resiliency of the upland forest to storms by shifting the seaward edge of the regeneration zone landward (Fagherazzi et al., 2019). Widespread hypersalinization occurs after storm surges flood low-gradient upland areas, promoting tree mortality, localized subsidence, and saltmarsh transgression (Williams et al., 1999; DeSantis et al., 2007; Fig. 9). Like the ecological ratchet model, our measurements of saltmarsh area from aerial photography show large increases in saltmarsh transgression rate and area during stormy periods when water levels are elevated frequently, followed by periods of little change as pocosin and wetland soils vertically accrete, despite SLR rates being persistently high. Modeled transgression rates at our sites were comparable to observed rates only during the paleo-quiescent period when rates were low (Fig. 7). During the rapid SLR period, most of the observed transgression rates were > modeled rates, including those that incorporate historical stormy decades in the measurement period at Long Bay (1957-2019 CE) and Nelson Bay (1957-1962 CE and 1962-2018 CE). Following inundation of the upland during a stormy period and formation of a ghost forest, shallow subsidence displaces the paleo-upland surface to a lower elevation forming a shallow step with the inflection point located at the edge of the persistence zone (Fig. 9). Local subsidence and changes in the depth of the paleo-upland surface at our sites make comparisons between modeled and observed transgression rates problematic. Measurements of vertical transgression that do not rely on upland slope but require the surface of the upland to be static during transgression (Fagherazzi et al., 2019; Schieder and Kirwan, 2019) are useful at sites where saltmarsh transgresses lithogenic sediments but are confounded by subsidence at our sites.

Transgression after a stormy period with frequent episodes of high water, is temporarily buffered from SLR by vertical accretion of upland soil (landward of inundation) and the shallow subsidence that formed a step between the paleo-upland surface and the surface of the persistence zone. Stormy periods effectively drive transgression ahead of what regional SLR would cause because of the associated localized subsidence. This is illustrated by the aerial photography record that shows rapid saltmarsh transgression from 1957-1970 CE at Nelson and Long bays followed by little change in saltmarsh area over the next few decades of rapid SLR. Upland forest vertical accretion rates can exceed the 0.9 mm yr^{-1} rate of SLR during the paleo-stormy period making storms a requirement for saltmarsh transgression at our sites.

During the paleo-stormy period, modeled transgression rates at both Jones and Long bays are high due to the low gradient of the paleo-upland surface. Those modeled transgression rates exceed the plotted observed values; however, those observed values are truly minimum rates due to overlapping basal saltmarsh peat age ranges at Jones Bay and the long duration over which transgression was measured at Long Bay (> 200 years) with 20% of the period including prior non-stormy conditions. In addition, the low rate of SLR during the paleo-stormy period contributes little to increasing storm surge through time and would isolate storm impacts to the same area. After the initial storms and associated increase in astronomical tidal range from inlet formation impacted the upland at the beginning of the paleo-stormy period, localized subsidence, a low rate of SLR, and vertical accretion of wetland soil in the persistence zone would make the upland highly resistant to further saltmarsh transgression (Fig. 9). Transgression is measured over millennial time scales during the paleo-stormy period when sea level was rising slowly as opposed to yearly to decadal time scales for the rapid SLR period, which effectively minimizes and maximizes the contribution of storms to the average observed transgression rate, respectively.

The stratigraphic records of saltmarsh strata are not preserving the same upland conditions that existed prior to transgression. Processes associated with the degradation of upland soil from salinization modify surface elevations during storms and SLR and displaced the paleo-upland surface to a lower elevation. Accelerating SLR can cross a threshold where vertical saltmarsh accretion cannot keep pace and large areas of saltmarsh become subtidal (Morris et al. 2002) and has been reported as one of the drivers responsible for the global decline in saltmarsh area (Kearney et al., 2002; Reed, 1995). Saltmarsh-area gain from upland transgression is thought to be capable of offsetting some losses and is often projected using numerical models (Fagherazzi et al., 2012). Model performance at the boundary between saltmarsh and low-gradient coastal uplands with hydric soils could be improved if both surge and shallow subsidence were included. Adding those contributing factors to models could result in a higher transgression rate than what would be predicted from SLR and slope. An increase in storm intensity and frequency and a decrease in tropical cyclone translation speed is predicted as the climate warms (Knutson et al., 2010; Colle et al., 2013; Emanuel, 2013; Villarini and Vecchi, 2013; Zhang and Colle, 2018) making it crucial to include storm impacts in models of saltmarsh transgression.

6. Conclusions

Core transects and aerial photos of low-gradient pocosin upland areas and fringing *Juncus* saltmarsh document variable transgression rates over the last 700 years. Saltmarsh transgression rates increased during stormy centuries and decades and when the rate of SLR increased from 0.9 mm yr^{-1} to 2.4 mm yr^{-1} at the end of the 19^{th} century. The lowest rates of transgression (~0.17 m yr^{-1}) occurred during a non-stormy period when the rate of SLR was only 0.9 mm yr^{-1}. During a paleo-stormy period with low rates of SLR, the vegetation of the lower upland area adjacent to saltmarsh was adversely affected by storm-generated wind and surge and an increase in astronomical tidal range associated with the formation of numerous tidal inlets. Those processes increased soil salinity and light penetration to the ground around the upland margin creating an environment that was harmful to pocosin vegetation and conducive for saltmarsh colonization. Storm-related stresses are necessary for saltmarsh transgression to progress across low-gradient vertically-accreting pocosin upland areas when the rate of SLR is low. Storms initiate transgression at these settings during slow SLR, even during non-stormy periods, but SLR is also important because it decreases the resilience of the upland forest to storm impacts and continually shifts storm surge landward promoting upland saltmarsh migration.

Predictions of saltmarsh transgression rates since 1335 CE, using a simple model based on the slope of the paleo-upland surface and the late Holocene sea-level curve, do not correspond well with observed transgression rates. Upland vertical accretion increases elevation and resistance to transgression; however, localized subsidence at the upland boundary from belowground root decay and compaction can generate elevation loss up to 2.0 cm yr^{-1}, which decreases through time. The elevation of the paleo upland, measured in the core transects, is not the same as it was prior to inundation and it is unclear if the slope is also modified. In low-gradient settings, a small change in slope causes a large change in predicted transgression rate. Furthermore, the saltmarsh that transgressed upland areas since 1957 CE is thicker than what can be explained by accommodation created only from the sea-level curve. This highlights the ability of saltmarsh to rapidly accrete and fill accommodation even at locations that are the furthest away from allogenic sediment sources. Human modifications of the upland-saltmarsh boundary, such as constructing developments and excavating ditches, are common and have increased with coastal populations. Changing the landscape around the edge of upland areas creates a barrier to saltmarsh transgression, whether it be from SLR or storms, and prevents losses of saltmarsh area at the shoreline to be offset by landward migration. Along low-gradient coastal areas, young saltmarsh that recently colonized the lower upland have high vertical accretion rates. By preventing new saltmarsh from forming on older upland soils we are losing an area of the marsh that likely would have some of the highest carbon accumulation rates.

Data Availability

Data for reproducing our results are available in supplemental information.

Author Contributions

CBM and ABR participated in all aspects of this study. MCB helped collect, process, and interpret data and edit the manuscript.

Acknowledgements

This research was supported by funding from North Carolina Sea Grant (grant number R/18-HCE-3). Jessamin Straub assisted in fieldwork, and Andrew McMains assisted with both field and laboratory work. Brent McKee and Emily Eidam provided valuable discussion and comments pertaining to this study.

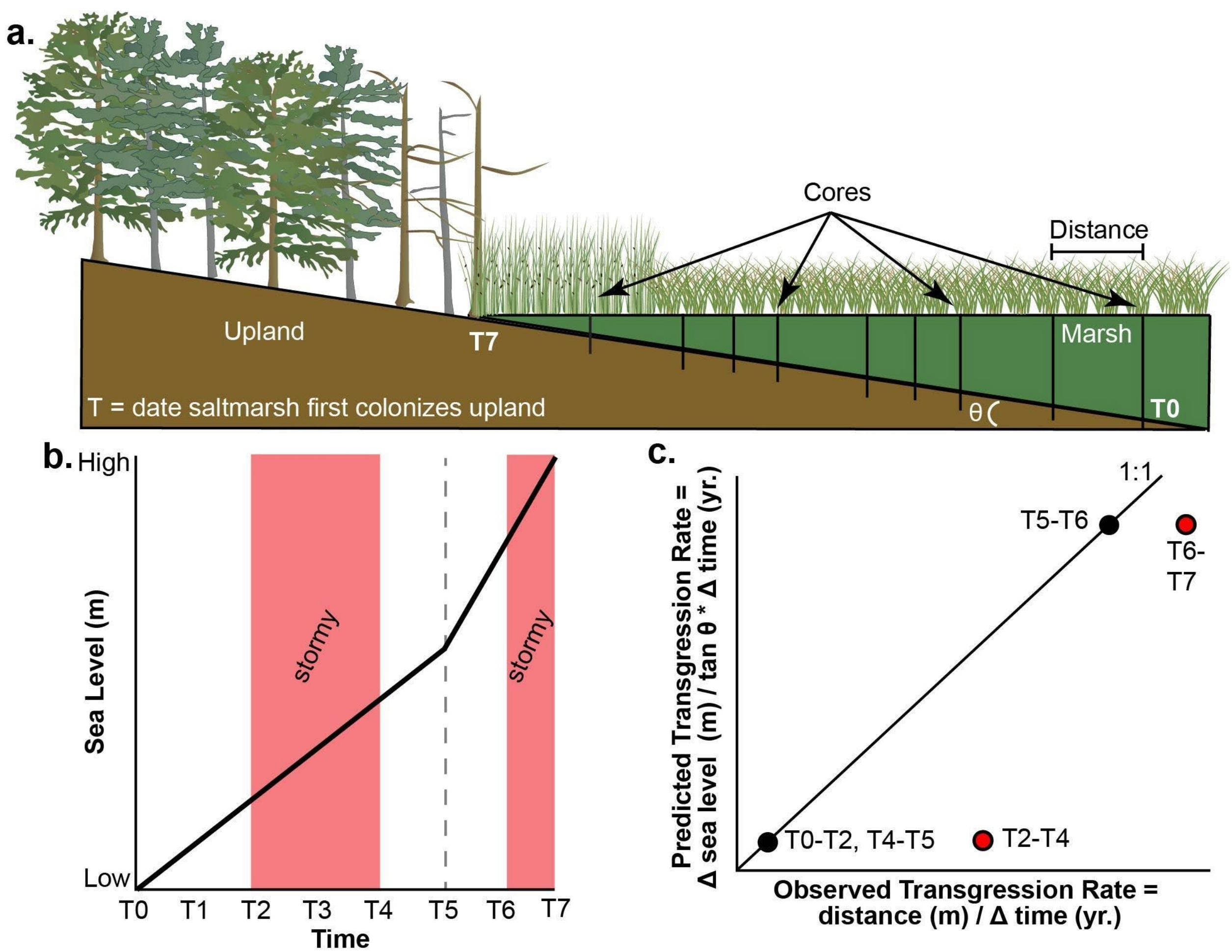

Figure 1. Conceptual model of saltmarsh transgression. The cross section shows saltmarsh transgression of an upland area with a constant slope. The date the first saltmarsh colonized the upland becomes younger in a landward direction (T0-T7; a.). The sea level curve for the period of saltmarsh transgression shows a constant rate of low SLR (T0-T5), a constant rate of rapid SLR (T5-T7) and two stormy periods T2-T4 and T6-T7 (red; b.). Given a fixed upland slope, the hypothesis is that observed transgression rates, based on the cross section, and predicted transgression rates, based on the sea level curve and upland slope, are equivalent (black circles) except during stormy periods (red circles) where other factors increase the rate above predicted.

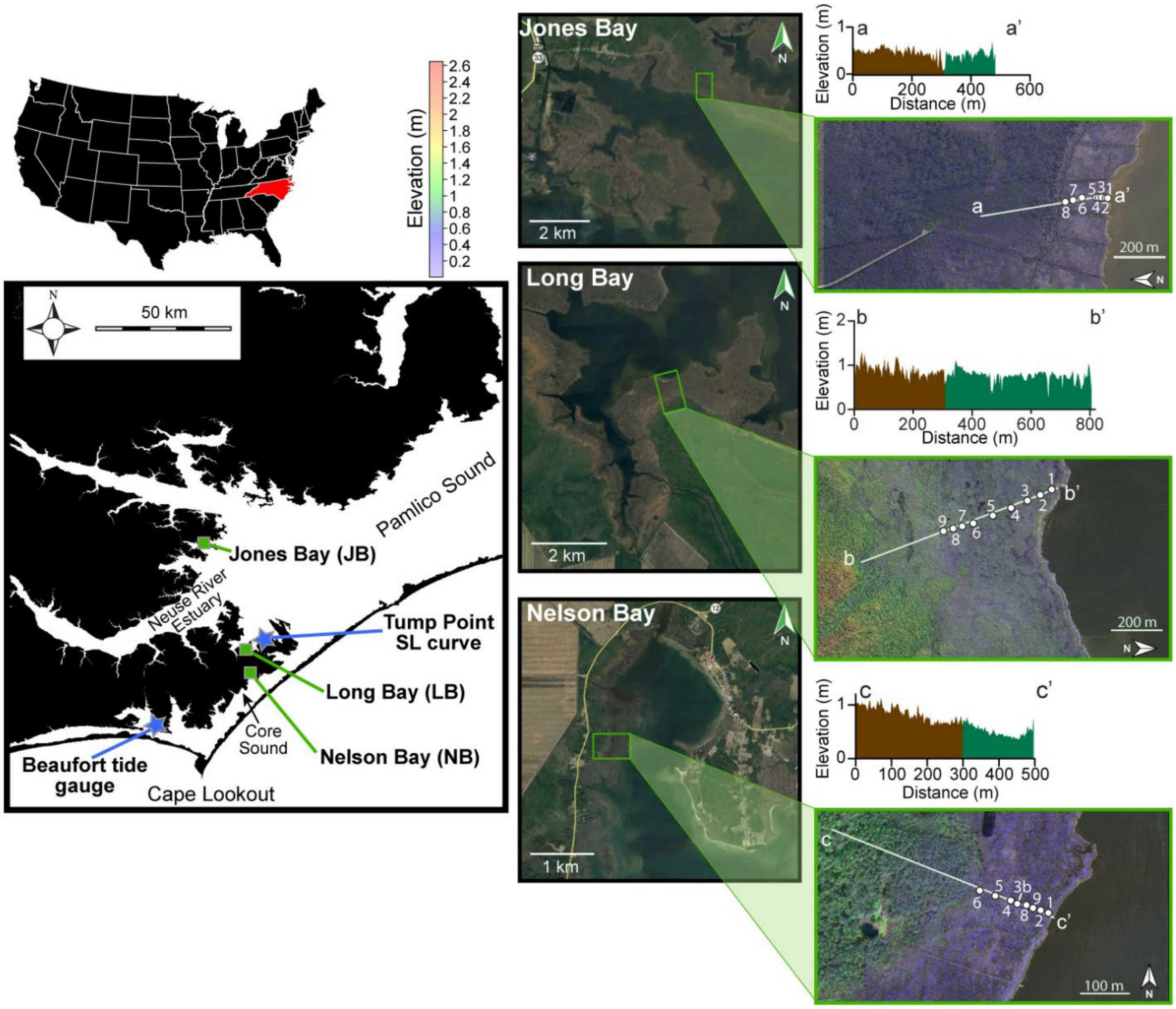

Figure 2. Study area map. Sample sites are located along the margins of Jones, Long, and Nelson bays. Core locations indicated as white circles. Elevation profiles are based on reprocessed LiDAR data and show the surface of the marsh (green) and upland (brown) along transect lines. All elevations relative to the NAVD88 datum.

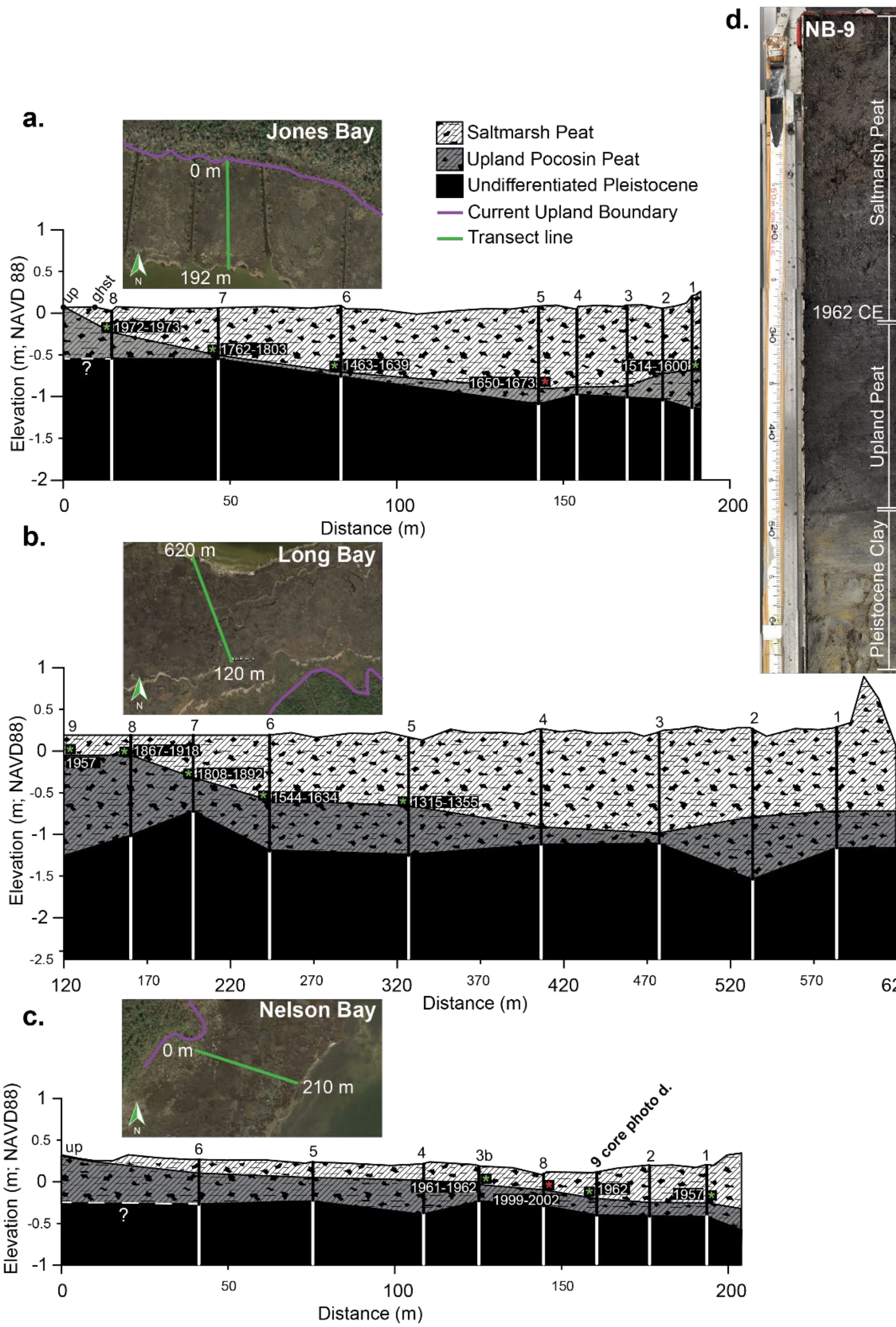

Figure 3. Stratigraphic cross sections. Aerial photos of the sample sites show locations of the transects at Jones Bay (a.), Long Bay (b.), and Nelson Bay (c.) extending from the upland-saltmarsh boundary (0 m) to the saltmarsh shoreline. Core locations identified by black vertical lines labeled by number, above. Representative core photo (d.) shows the general appearance of the three units sampled in the cores from each site. Asterisks mark radiocarbon samples and relevant date ranges (green or red for those used or excluded in our analysis, respectively). See Table 1 for additional information on radiocarbon dates.

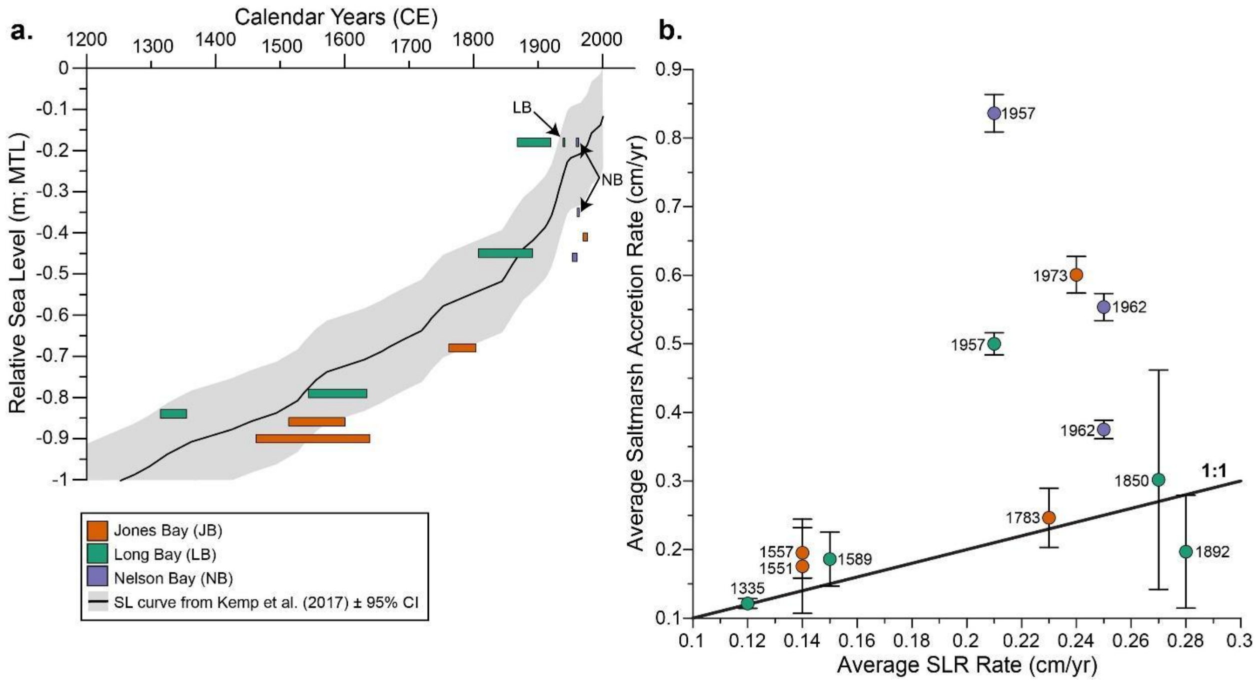

Figure 4. Calibrated radiocarbon date ranges of the basal saltmarsh peat samples used in the study overlain on the Kemp et al. (2017) sea-level curve from Tump Point, NC (a.). The width of the date-range boxes is the 2-cm vertical sampling interval. Average saltmarsh accretion rate, based on the date range of the basal saltmarsh peat and the core-collection date, versus the average rate of SLR, based on the Kemp et al. (2017) sea-level curve (b.). Symbols mark the average accretion rate using the median date (± based on max. and min. saltmarsh age) and the average rate of sea-level rise calculated by linear regression through sea-level data points from the median date to 2000 CE.

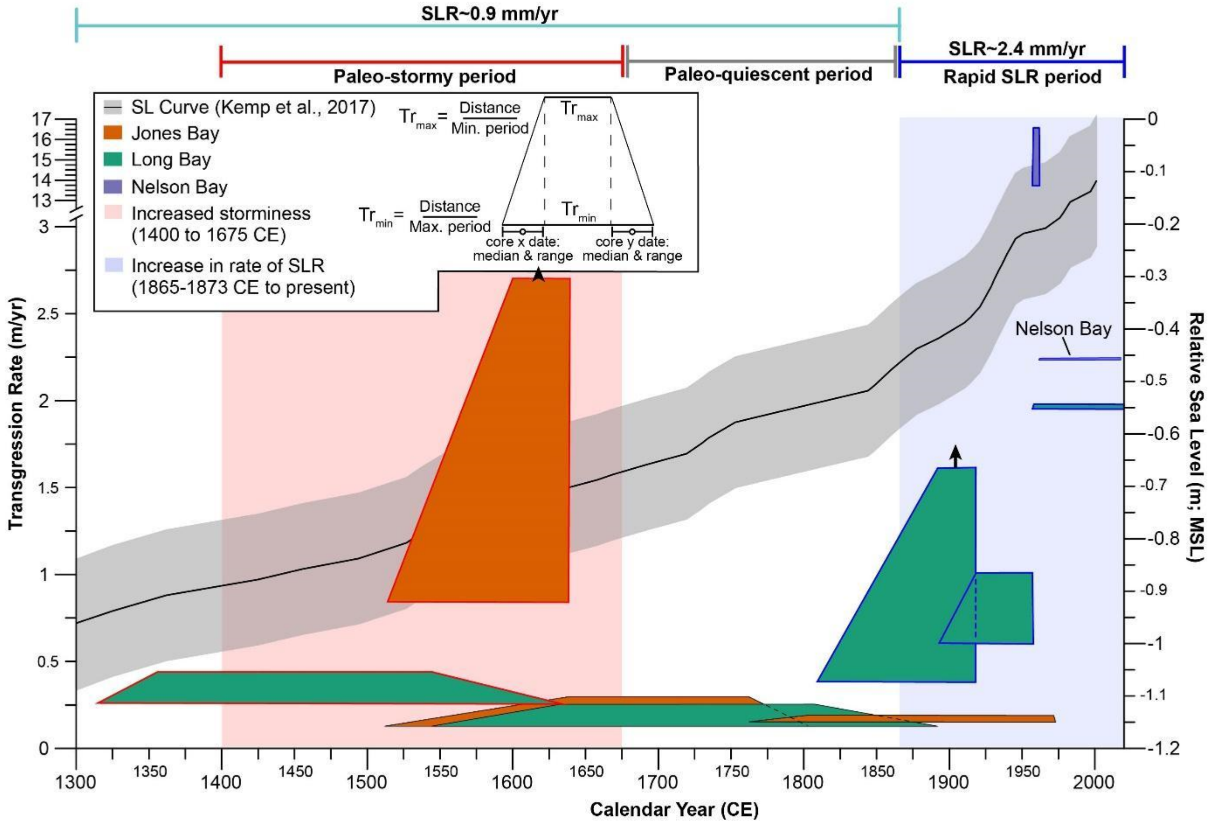

Figure 5. Transgression rates vary through time at each site. Rates are measured between cores and plotted as trapezoids to illustrate the range of possible transgression rates from the radiocarbon date ranges (Table 1). Transgression rates (Tr) are calculated over the time periods depicted by the width of Tr_{max} and Tr_{min}. Vertical arrows indicate that the date ranges of basal saltmarsh peat overlap and the maximum transgression rate (Tr_{max}) could be higher than what is plotted.

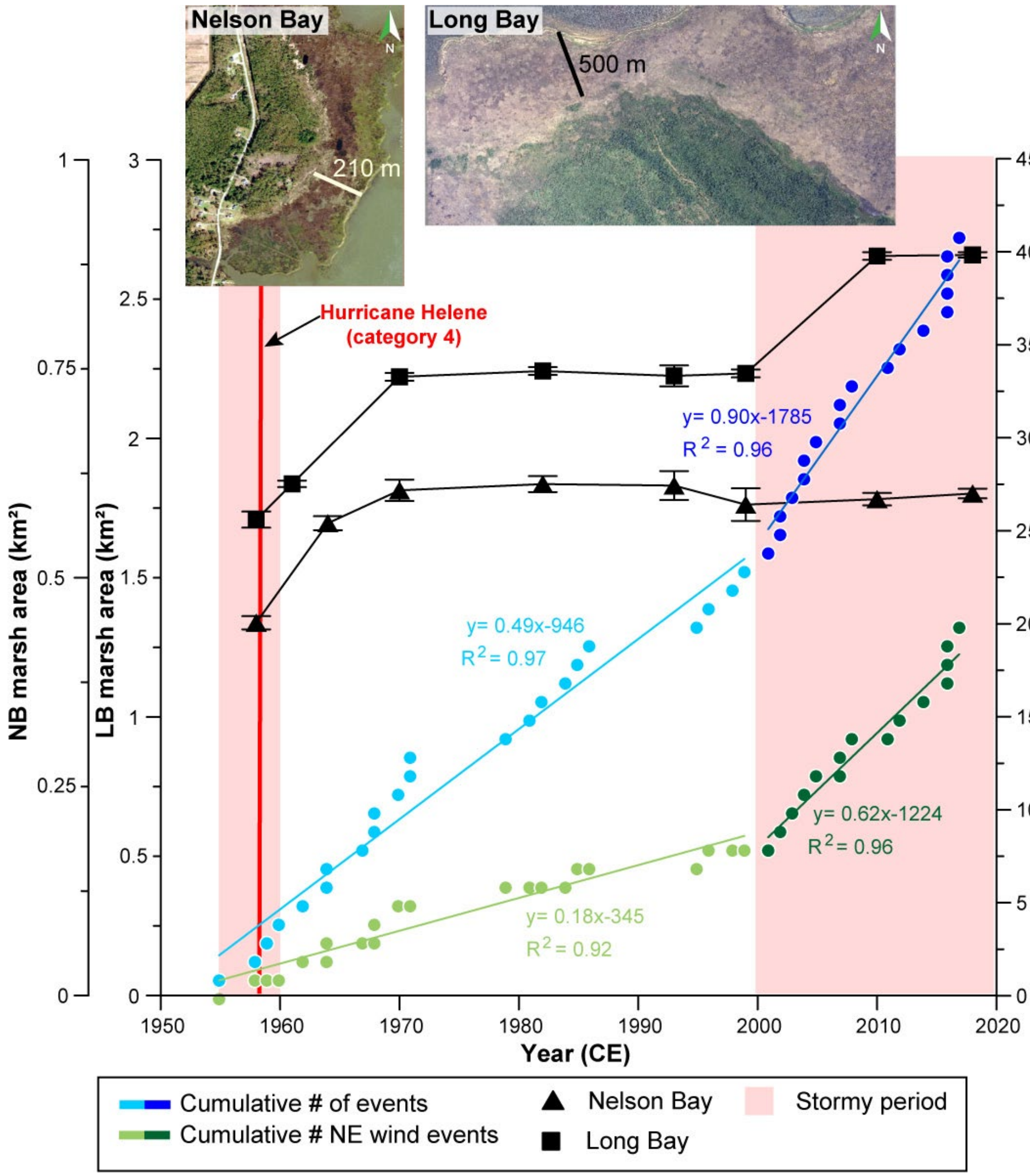

Figure 6. Change in saltmarsh area at the Long and Nelson bay sites and the historical storm record for the area since 1957 CE. The saltmarsh area was digitized using the coverage shown in the aerial photos (above) with the location of the coring transect (black or white line) indicated for scale. The cumulative number of events (blue) includes all storms with wind > 55.5 km hr^{-1}, the cumulative number of NE wind events (green) includes winds > 55.5 km hr^{-1} that are dominantly out of the NE quadrant, and major hurricane Helene (red) was associated with numerous high-water events 1954-1960. Slopes of the linear regressions show that there were more storms post 2000 CE (p value << 0.0005 for all events and NE wind events).

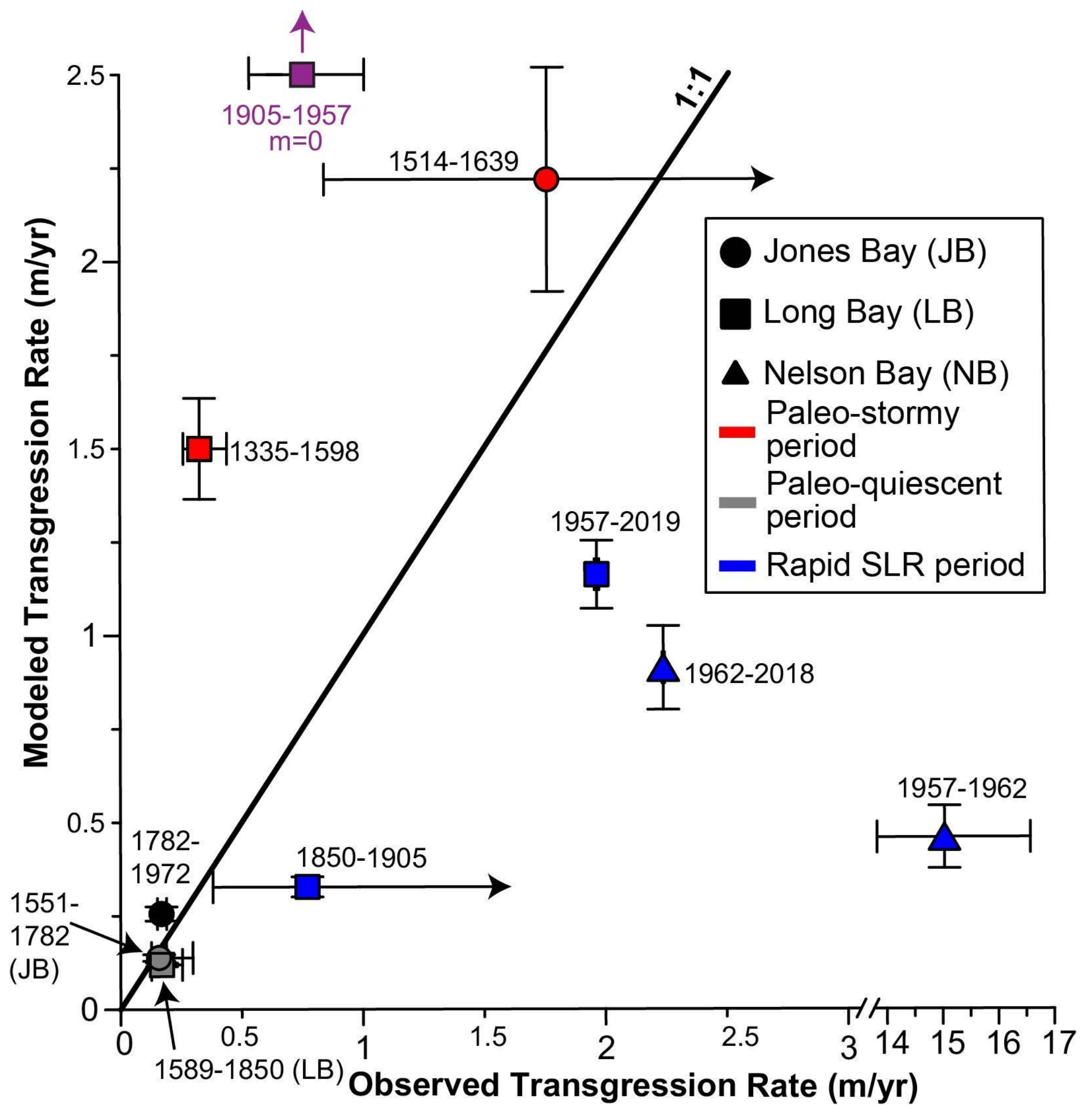

Figure 7. Modeled versus observed transgression rates for each period measured at the sites using stratigraphic data. Observed transgression rate is the median rate with error based on the maximum and minimum period, which is equivalent to 0.5 times the height of the trapezoids shown on Figure 5. Modeled transgression rate for the period is calculated from sea-level rise and the paleo-upland slope with error based on the 95% confidence interval of the regression line through sea-level data points sampled from the Kemp et al. (2017) sea-level curve. The purple point only depicts the observed transgression rate because the paleo-upland slope between the two cores from which the measurement was made is indistinguishable from zero. The period over which the black Jones Bay point represents could not be classified.

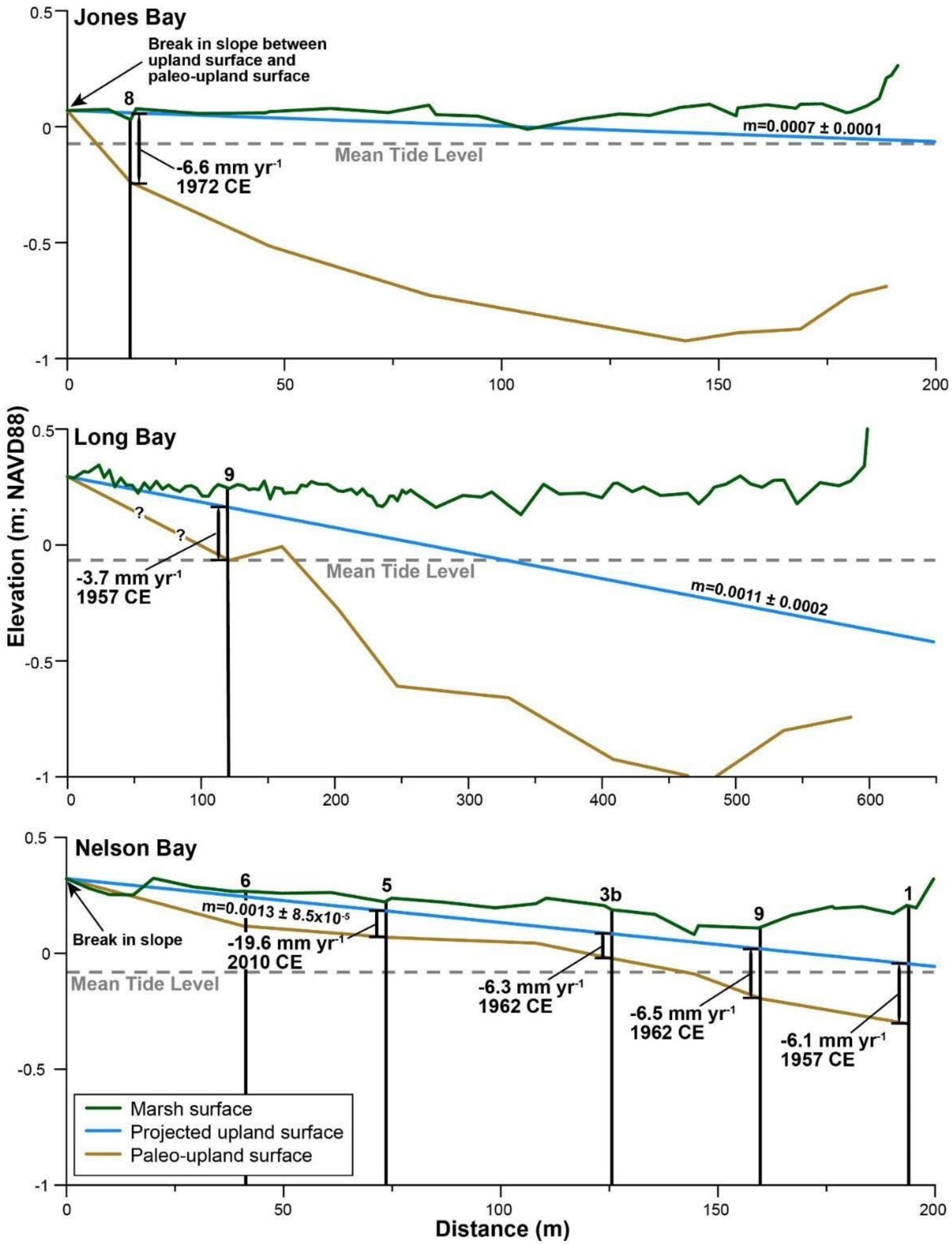

Figure 8. The upland-surface gradient (blue) projected into the saltmarsh at each transect site. The location and extent of the transects are the same as shown in Figure 3. The projected upland surface is based on a linear regression (± the 95% CI) through the upland portion of the elevation profiles shown in Figure 2. Vertical black lines indicate locations of cores with basal saltmarsh peat ages postdating 1957 CE. Estimated shallow-subsidence rate, labeled adjacent to each core, is the distance between the paleo-upland surface and the projected upland surface divided by the age of the saltmarsh. Saltmarsh age is based on the date saltmarsh first colonized the location to 2018 CE.

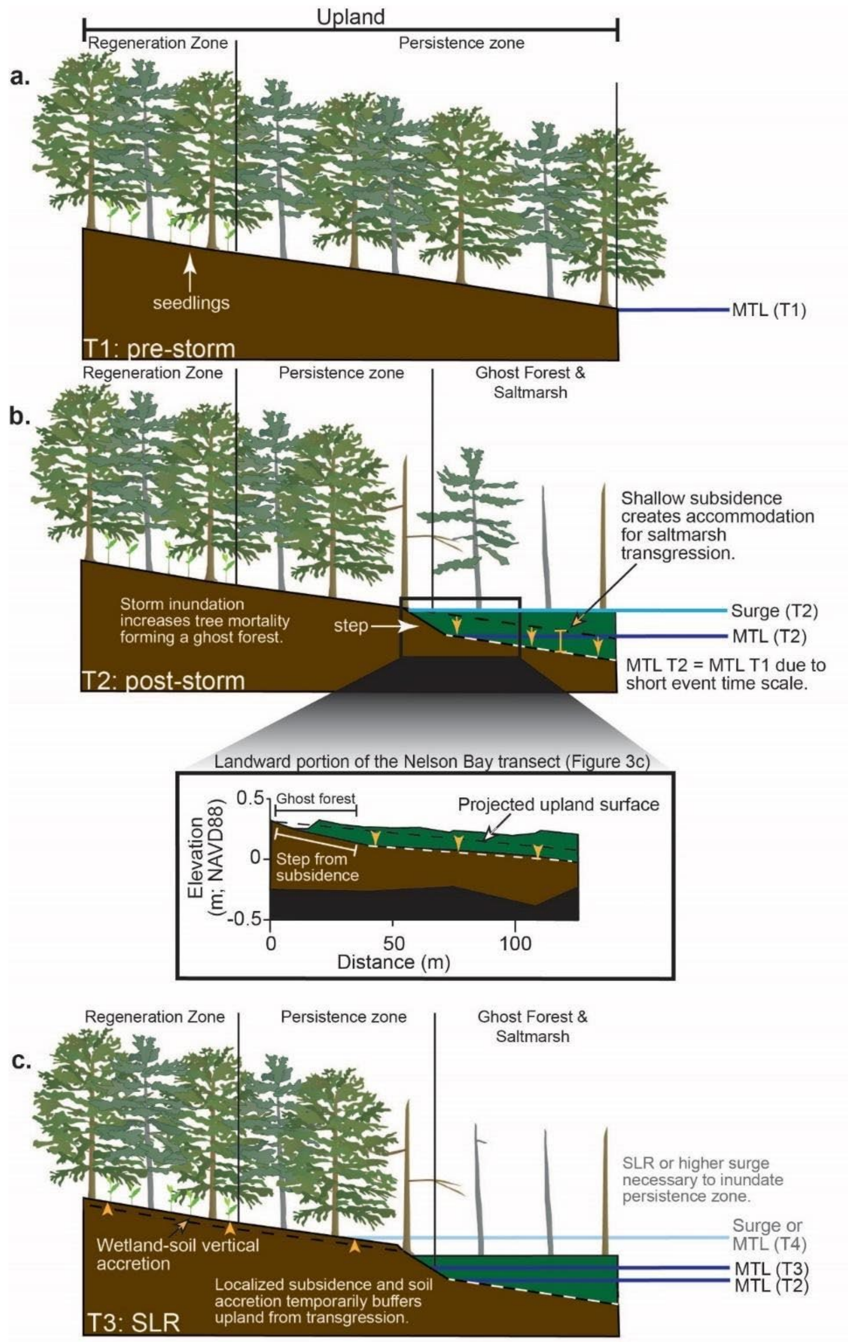

Figure 9. Conceptual model describing saltmarsh transgression of the coastal plain. The upland at time 1 (T1) prior to transgression (a.). During a storm (T2), surge (light blue) inundates the persistence zone, increases tree mortality, and forms a ghost forest. Decay and compaction of upland organic material displaces the paleo-upland surface to a lower elevation forming a step and promoting transgression (b.). The Nelson Bay transect shows the step between the subsiding paleo-upland surface and the surface of the persistence zone. Mean tide level (MTL) increases with SLR during a subsequent non-stormy period (T3) but causes no additional transgression because of wetland soil vertical accretion and localized subsidence. A subsequent storm or accelerated SLR (T4) is necessary to progress transgression.

Table 1. Basal saltmarsh peat dates

Core	Basal saltmarsh elevation (m; MTL)	Sample Interval (cm)	Fraction Modern ± Error	Radiocarbon Date ± Error (years BP)	Calibrated Date Range (years CE)	Certainty
JB1	-0.859	88-90	0.9618±0.0020	315±15	1514-1600	0.78
JB5	-1.094	99-101	0.9736±0.0020	215±15	1650-1673†	0.375
JB6	-0.897	80-82	0.9579±0.0042	345±35	1463-1639 1514-1639*	1
JB7	-0.685	56-58	0.9760±0.0019	195±15	1762-1803	0.49
JB8	-0.41	25-27	1.457±0.0031	n/a	1972.21-1973.87	0.731
LB5	-0.839	81-83	0.9323±0.0020	565±20	1315-1335	0.542
LB6	-0.789	78-80	0.9585±0.0019	340±15	1544-1634	0.655
LB7	-0.456	49-51	0.9861±0.0021	115±15	1808-1892	0.605
LB8	-0.187	23-25	0.9905±0.0026	75±20	1867-1918 1892-1918*	0.53
LB9	-0.187	29-31	1.0697±0.0023	n/a	1957.1-1957.7	0.095
NB1	-0.463	50-51	1.0694±0.0021	n/a	1957.1-1957.69	0.097
NB9	-0.356	29-31	1.3672±0.0038	n/a	1962.41-1962.73	0.129
NB8	-0.249	15-17	1.0913±0.0022	n/a	1999.85-2002.06†	0.889
NB3b	-0.182	19-21	1.271±0.0026	n/a	1961.79-1962.05	0.115

Core names have been shortened to JB (Jones Bay), LB (Long Bay), and NB (Nelson Bay).
* Truncated date range used in transgression rate calculations. Corrected for overlap with adjacent core.
† excluded from study

REFERENCES CITED

Airoldi, L., Beck, M. (2007). Loss, status and trends for coastal marine habitats of Europe. Boca Raton: CRC Press-Taylor & Francis group, 345-405.

Altieri, A. H., Bertness, M. D., Coverdale, T. C., Herrmann, N. C., Angelini, C. (2012). A trophic cascade triggers collapse of a salt-marsh ecosystem with intensive recreational fishing. *Ecology*, *93*(6), 1402–1410.

Baily, B., Pearson, A. W. (2007). Change Detection Mapping and Analysis of Salt Marsh Areas of Central Southern England from Hurst Castle Spit to Pagham Harbour. *Journal of Coastal Research*, *236*(236), 1549–1564.

Barbier, E.B. (2011). The value of estuarine and coastal ecosystem services. *Ecological Monographs, 81*(2), 169-193.

Barbier, E.B., Koch, E.W., Silliman, B.R., Hacker, S.D., Wolanski, E., Primavera, J., Granek, E.F., Polasky, S., Aswani, S., Cramer, L.A., Stoms, D.M., Kennedy, C.J., Bael, D., Kappel, C.V., Perillo, G.M.E., Reed, D.J. (2008). Coastal Ecosystem-Based Management with Nonlinear Ecological Functions and Values. *Science, 319*(5861), 321-323.

Bertness, M.D. (1988). Peat accumulation and the success of marsh plants. *Ecology, 69*, 703-713.

Bertness, M.D., Ewanchuk, P.J., Silliman, B.R. (2002). Anthropogenic modification of New England salt marsh landscapes. *Proceedings of the National Academy of Sciences, 99*(3), 1395-1398.

Blood, E., Anderson, P., Smith, P. A., Nybro, C., Ginsberg, K. . A. . (1991). Effects of Hurricane Hugo on Coastal Soil Solution Chemistry in South Carolina. *Biotropica*, *23*(4), 348–355.

Bricker-Urso, S., Nixon, S. W., Cochran, J. K., Hirschberg, D. J., Hunt, C. (1989). Accretion Rates and Sediment Accumulation in Rhode Island Salt Marshes. *Estuaries, 12*(4), 300–317.

Brinson, M. M. (1991). Landscape properties of pocosins and associated wetlands. *Wetlands*, *11*(1), 441–465.

Brinson, M.M, Christian, R.R., Blum, L.K. (1995). Multiple states in the sea-level induced transition from terrestrial forest to estuary. *Coastal and Estuarine Research Federation, 18*(4), 648-659.

Bromberg, K.D., Bertness, M.D. (2005). Reconstructing New England salt marsh losses using historical maps. *Estuaries, 28*(6), 823-832.

Cahoon, D. R., Hensel, P. F., Spencer, T., Reed, D. J., McKee, K. L., Saintilan, N. (2006). Coastal Wetland Vulnerability to Relative Sea-Level Rise: Wetland Elevation Trends and Process Controls. *Wetlands and Natural Resource Management*, *190*, 271–292.

CEC, 2016. North America's Blue Carbon: Assessing Seagrass, Salt Marsh and Mangrove Distribution and Carbon Sinks, Commission for Environmental Cooperation, Montreal.

Coleman, J. M., Smith, W. G. (1964). Late recent rise of sea level. *Geological Society of America Bulletin, 75*, 833–840.

Colle, B.A., Zhang, Z., Lombardo, K.A., Chang, E., Liu, P., Zhang, M., 2013. Historical Evaluation and Future Prediction of Eastern North American and Western Atlantic Extratropical Cyclones in the CMIP5 Models during the Cool Season. Journal of Climate 26, 6882-6903.

Charles, S. P., Kominoski, J. S., Troxler, T. G., Gaiser, E. E., Servais, S., Wilson, B. J., Rudnick, D. T. (2019). Experimental Saltwater Intrusion Drives Rapid Soil Elevation and Carbon Loss in Freshwater and Brackish Everglades Marshes. *Estuaries and Coasts*, *42*(7), 1868–1881.

Chmura, G. L., Hung, G. A. (2004). Controls on salt marsh accretion: A test in salt marshes of eastern Canada. *Estuaries*, *27*(1), 70–81. https://doi.org/10.1007/BF02803561

Christian, R. R., Bryant, W. L., Brinson, M. M. (1990). Juncus roemerianus production and decomposition along gradients of salinity and hydroperiod. *Marine Ecology Progress Series*, *68*, 137–145.

Crosby, S. C., Sax, D. F., Palmer, M. E., Booth, H. S., Deegan, L. A., Bertness, M. D., Leslie, H. M. (2016). Salt marsh persistence is threatened by predicted sea-level rise. *Estuarine, Coastal and Shelf Science*, *181*, 93–99.

Culver, S. J., Horton, B. P. (2005). Infaunal marsh foraminifera from the outer banks, North Carolina, U.S.A. *Journal of Foraminiferal Research*, *35*(2), 148–170.

Davis, C.A. (1910). Salt marsh formation near Boston and its geological significance. Economic *Geology, 5*(7), 623-639.

DeLaune, R. D., Nyman, J. A., Patrick, W. H. (1994). Peat Collapse , Ponding and Wetland Loss in a Rapidly Submerging Coastal Marsh. *Journal of Coastal Research*, *10*(4), 1021–1030.

DeSantis, L. R. G., Bhotika, S., Williams, K., Putz, F. E. (2007). Sea-level rise and drought interactions accelerate forest decline on the Gulf Coast of Florida, USA. *Global Change Biology*, *13*(11), 2349–2360.

Doody, J.P. (2013). Coastal squeeze and managed realignment in southeast England, does it tell us anything about the future? *Ocean & Coastal Management, 79*(0), 34-41.

Donnelly, J. P., Bertness, M. D. (2001). Rapid shoreward encroachment of salt marsh cordgrass in response to accelerated sea-level rise. *Proceedings of the National Academy of Sciences of the United States of America*, *98*(25), 14218–14223.

Donnelly, J.P., Hawkes, A.D., Lane, P., MacDonald, D., Shuman, B.N., Toomey, M.R., van Hengstum, P.J., Woodruff, J.D. (2015). Climate forcing of unprecedented intense-hurricane activity in the last 2000 years. *Earth's Future, 3*(2), 49-65.

Doyle, T.W., Krauss, K.W., Conner, W.H., From, A.S. (2010) Predicting the retreat and migration of tidal forests along the northern Gulf of Mexico under sea-level rise. *Forest Ecology and Management 259*(4) 770-777.

Drexler, J. Z., Fuller, C. C., Orlando, J., Salas, A., Wurster, F. C., Duberstein, J. A. (2017). Estimation and Uncertainty of Recent Carbon Accumulation and Vertical Accretion in Drained and Undrained Forested Peatlands of the Southeastern USA. *Journal of Geophysical Research: Biogeosciences*, *122*(10), 2563–2579.

Duarte, C. M., Dennison, W. C., Orth, R. J. W., Carruthers, T. J. B. (2008). The charisma of coastal ecosystems: Addressing the imbalance. *Estuaries and Coasts*, *31*(2), 233–238.

Emanuel, K.A., 2013. Downscaling CMIP5 climate models shows increased tropical cyclone activity over the 21st century. Proc Natl Acad Sci U S A 110, 12219-12224.

Engelhart, S. E., Horton, B. P. (2012). Holocene sea level database for the Atlantic coast of the United States. *Quaternary Science Reviews*, *54*, 12–25.

Enwright, N. M., Griffith, K. T., Osland, M. J. (2016). Barriers to and opportunities for landward migration of coastal wetlands with sea-level rise. *Frontiers in Ecology and the Environment 14,* 307-316.

Everett, T., Chen, Q., Karimpour, A., Twilley, R. (2019). Quantification of Swell Energy and Its Impact on Wetlands in a Deltaic Estuary. *Estuaries and Coasts 42,* 68-84.

Fagherazzi, S., Kirwan, M. L., Mudd, S. M., Guntenspergen, G. R., Temmerman, S., D'Alpaos, A., van de Koppel, J., Rybczyk, J.M., Reyes, E., Craft, C., Clough, J. (2012). Numerical models of salt marsh evolution: Ecological, geomorphic, and climatic factors. *Reviews of Geophysics*, *50*(1).

Fagherazzi, S., Anisfeld, S. C., Blum, L. K., Long, E. V., Feagin, R. A., Fernandes, A., Williams, K. (2019). Sea level rise and the dynamics of the marsh-upland boundary. *Frontiers in Environmental Science*, *7*, 1–18.

Farron, S.J., Hughes, Z.J., Fitzgerald, D.M., 2020. Assessing the response of the Great Marsh to sea-level rise: Migration, submersion or survival. Marine Geology 425, 106195.

Feagin, R.A., Martinez, M.L., Mendoza-Gonzalez, G., Costanza, R., (2010). Salt marsh zonal migration and ecosystem service change in response to global sea level rise: a case study from an urban region. *Ecology and Society, 15*(4), 14.

FitzGerald, D. M., Fenster, M. S., Argow, B. A., Buynevich, I. V. (2008). Coastal Impacts Due to Sea-Level Rise. *Annual Review of Earth and Planetary Science*, *23*(2), 175–192.

Gardner, L. R., Michener, W. K., Blood, E. R., Williams, T. M., Lipscomb, D. J., Jefferson, W. H. (1991). Ecological impact of Hurricane Hugo - salinization of a coastal forest. *Journal of Coastal Research, Special Issue*, *8*(8), 301–317.

Gardner, L.R., Porter, D.E. (2001). Stratigraphy and geologic history of a southeastern salt marsh basin, North Inlet, South Carolina, USA. *Wetlands Ecology and Management, 9*(5), 371-385.

Gedan, K.B., Silliman, B.R., Bertness, M.D. (2009). Centuries of human-driven change in salt marsh ecosystems. *Annual Reviews of Marine Science, 1*(1), 117-141.

Gehrels, W. R. (1994). Determining Relative Sea-Level Change from Salt-Marsh Foraminifera and Plant Zones on the Coast of Maine , U.S.A.. *Journal of Coastal Research*, *10*(4), 990–1009.

Giese, G.L., Wider, H.B., Parker Jr., G.G. (1985). Hydrology of major estuaries and sounds of North Carolina. US Geological Survey Water Supply Paper. USGS, Reston, VA, 108 pp.

Gonneea, M. E., Maio, C. V., Kroeger, K. D., Hawkes, A. D., Mora, J., Sullivan, R., Madsen, S., Buzard, R.M., Cahill, N., Donnelly, J. P. (2019). Salt marsh ecosystem restructuring enhances elevation resilience and carbon storage during accelerating relative sea-level rise. *Estuarine, Coastal and Shelf Science*, *217*, 56–68.

Goodbred, S. L., Wright, E. E., Hine, A. C. (1998). Sea-level change and storm-surge deposition in a late holocene florida salt marsh. *Journal of Sedimentary Research, Section B: Stratigraphy and Global Studies*, *68*(2), 240–250.

Graham, S. A., Mendelssohn, I. A. (2014). Coastal wetland stability maintained through counterbalancing accretionary responses to chronic nutrient enrichment. *Ecology 95,* 3271-3283.

Herbert, E. R., Boon, P., Burgin, A. J., Neubauer, S. C., Franklin, R. B., Ardon, M., Langley, J. A. (2015). A global perspective on wetland salinization: Ecological consequences of a growing threat to freshwater wetlands. *Ecosphere*, *6*(10), 1–43.

Hess, K.W., Spargo, E.A., Wong, A., White, S.A., Gill, S.K. (2005). VDatum for Central Coastal North Carolina Tidal Datums, Marine Grids, and Sea Surface Topography. National Oceanic and Atmospheric Administration, p. 46.

Horton, B. P., Culver, S. J. (2008). Modern Intertidal Foraminifera of the Outer Banks, North Carolina, U.S.A., and their Applicability for Sea-Level Studies. *Journal of Coastal Research*, *245*(May), 1110–1125.

Howes, N. C., FitzGerald, D. M., Hughes, Z. J., Georgiou, I. Y., Kulp, M. A., Miner, M. D., Smith, J. M., Barras, J. A. (2010). Hurricane-induced failure of low salinity wetlands. *Proceedings of the National Academy of Sciences of the United States of America*, *107*(32), 14014–14019.

Johnson, D.W. (1919) Shore processes and shoreline development. John Wiley & Sons, Incorporated, Boston, 584 p.

Kearney, M. S., Rogers, A. S., Townshend, J. R. G., Rizzo, E., Stutzer, D., Stevenson, J. C., Sundborg, K. (2002). Landsat imagery shows decline of coastal marshes in Chesapeake and Delaware bays. *Eos, 83*(16), 173–184.

Kemp, A. C., Horton, B. P., Culver, S. J. (2009). Distribution of modern salt-marsh foraminifera in the Albemarle-Pamlico estuarine system of North Carolina, USA: Implications for sea-level research. *Marine Micropaleontology*, *72*(3–4), 222–238.

Kemp, A. C., Horton, B. P., Culver, S. J., Corbett, D. R., van de Plassche, O., Gehrels, W. R., Parnell, A. C. (2009). Timing and magnitude of recent accelerated sea-level rise (North Carolina, United States). *Geology*, *37*(11), 1035–1038.

Kemp, A. C., Horton, B. P., Donnelly, J. P., Mann, M. E., Vermeer, M., Rahmstorf, S. (2011). Climate related sea-level variations over the past two millennia. *Proceedings of the National Academy of Sciences*, *108*(27), 11017–11022.

Kemp, A.C., Kegel, J.J., Culver, S.J., Barber, D.C., Mallinson, D.J., Leorri, E., Bernhardt, C.E., Cahill, N., Riggs, S.R., Woodson, A.L., Mulligan, R.P., Horton, B.P. (2017). Extended late Holocene relative sea-level histories for North Carolina, USA. *Quaternary Science Reviews, 160*, 13-30.

Kennish, M.J. (2001). Coastal Salt Marsh Systems in the U.S.: A Review of Anthropogenic Impacts. *Journal of Coastal Research, 17*(3), 731-748.

Kirwan, M., Temmerman, S. (2009). Coastal marsh response to historical and future sea-level acceleration. *Quaternary Science Reviews*, *28*(17-18), 1801-1808.

Kirwan, M. L., Guntenspergen, G. R., D'Alpaos, A., Morris, J. T., Mudd, S. M., Temmerman, S. (2010). Limits on the adaptability of coastal marshes to rising sea level. *Geophysical Research Letters*, *37*(23), 1–5.

Kirwan, M.L., Walters, D.C., Reay, W.G., Carr, J.A. (2016). Sea level driven marsh expansion in a coupled model of marsh erosion and migration. *Geophysical Research letters, 43*(9), 4366-4373.

Knutson, T. R., McBride, J. L., Chan, J., Emanuel, K., Holland, G., Landsea, C., Held, I., Kossin, J.P., Srivastava, A.K., Sugi, M. (2010). Tropical cyclones and climate change. *Nature Geoscience*, *3*(3), 157–163.

Kozlowski, T. T. (1997). Responses of woody plants to flooding and salinity. *Tree Physiology*, *17*(7), 490–490.

Langston, A.K., Durán Vinent, O., Herbert, E.R., Kirwan, M.L., 2020. Modeling long-term salt marsh response to sea level rise in the sediment-deficient Plum Island Estuary, MA. Limnology and Oceanography 65, 2142-2157.

Leonardi, N., Ganju, N. K., Fagherazzi, S. (2016). A linear relationship between wave power and erosion determines salt-marsh resilience to violent storms and hurricanes. *Proceedings of the National Academy of Sciences of the United States of America*, *113*(1), 64–68.

Lotze H.K., Lenihan H.S., Bourque B.J., Bradbury R.H., Cooke R.G., Kay M.C., Kidwell S.M., Kirby M.X., Peterson C.H., Jackson J.B. (2006). Depletion, degradation and recovery potential of estuaries and coastal seas. *Science 312*(5781):1806–1809.

Luettich Jr, R. A., Carr, S. D., Reynolds-Fleming, J. V., Fulcher, C. W., McNinch, J. E. (2002). Semi-diurnal seiching in a shallow, micro-tidal lagoonal estuary. *Continental Shelf Research*, *22*(11-13), 1669-1681.

Mallinson, D.J., Smith, C.W., Mahan, S., Culver, S.J., McDowell, K. (2011). Barrier island response to late Holocene climate events, North Carolina, USA. *Quaternary Research, 76*(1), 46-57.

McLeod, E., Chmura, G. L., Bouillon, S., Salm, R., Björk, M., Duarte, C. M., Silliman, B. R. (2011). A blueprint for blue carbon: Toward an improved understanding of the role of vegetated coastal habitats in sequestering CO2. *Frontiers in Ecology and the Environment*, *9*(10), 552–560.

McTigue, N., Davis, J., Rodriguez, A. B., McKee, B., Atencio, A., Currin, C. (2019). Sea Level Rise Explains Changing Carbon Accumulation Rates in a Salt Marsh Over the Past Two Millennia. *Journal of Geophysical Research: Biogeosciences*, *124*(10), 2945–2957.

Michener, W. K., Blood, E. R., Bildstein, K. L., Brinson, M. M., Gardner, L. R. (1997). Climate change, hurricanes and tropical storms, and rising sea level in coastal wetlands. *Ecological Applications*, *7*(3), 770–801.

Moller, I., Kudella, M., Rupprecht, F., Spencer, T., Paul, M., van Wesenbeeck, B.K., Wolters, G., Jensen, K., Bouma, T.J., Miranda-Lange, M., Schimmels, S. (2014). Wave attenuation over coastal salt marshes under storm surge conditions. *Nature Geoscience, 7*(10), 727-731.

Moorhead, K. K., Brinson, M. M. (1995). Response of Wetlands to Rising Sea Level in the Lower Coastal Plain of North Carolina. *Ecological Applications*, *5*(1), 261–271.

Morris, J. T., Sundareshwar, P. V., Nietch, C. T., Kjerfve, B. Cahoon, D. R. (2002). Responses of coastal wetlands to rising sea level. *Ecology, 83*, 2869–2877.

Mulligan, R. P., Mallinson, D. J., Clunies, G. J., Rey, A., Culver, S. J., Zaremba, N., Mitra, S. (2019). Estuarine Responses to Long-Term Changes in Inlets, Morphology, and Sea Level Rise. *Journal of Geophysical Research: Oceans*, *124*(12), 9235–9257.

Neumeier, U., Ciavola, P. (2004). Flow Resistance and Associated Sedimentary Processes in a Spartina maritima Salt-Marsh. *Journal of Coastal Research*, *202*(2), 435–447.

National Oceanic and Atmospheric Administration (2013). National Coastal Population Report: Population trends from 1970-2020. NOAA, Department of Commerce.

National Oceanic and Atmospheric Administration Data Access Viewer. (Date accessed 5/10/2019). https://coast.noaa.gov/dataviewer/#/

National Oceanic and Atmospheric Administration Historical Hurricane Tracks. (Date accessed 7/10/2019). https://oceanservice.noaa.gov/news/historical-hurricanes/

Oertel, G. F., Woo, H. J. (1994). Landscape Classification and Terminology for Marsh in Deficit Coastal Lagoons. *Journal of Coastal Research*, *10*(4), 919–932.

Ouyang, X., Lee, S.Y. (2014). Updated estimates of carbon accumulation rates in coastal marsh sediments. *Biogeosciences* 11, 5057-5071.

Pethick, J. (2001). Coastal management and sea-level rise. *Catena, 42* (2-4) 307-322.

Peterson, G. W., Turner, R. E. (1994). The value of salt marsh edge vs interior as a habitat for fish and decapod crustaceans in a Louisiana tidal marsh. *Estuaries*, *17*(1), 235–262.

Pontee, N. (2013). Defining coastal squeeze: A discussion. *Ocean & Coastal Management, 84*, 204-207.

Prouty, W. F. (1952). Carolina bays and their origin. *Geological Society of America Bulletin*, *63*(2), 167-224.

Raabe, E.A., Stumpf, R.P. (2016). Expansion of tidal marsh in response to sea-level rise: Gulf Coast of Florida, USA. *Estuaries and Coasts, 39*(1), 145-157.

Redfield, A. (1965). Ontogeny of a Saltmarsh Estuary. *Science*, *147*(3653), 50–55.

Redfield, A., Rubin, M. (1962). The Age of Salt Marsh Peat and Its Relation to Recent Changes in Sea Level at Barnstable, Massachusetts. *Proceedings of the National Academy of Sciences of the United States of America*, *48*(10), 1728–1735.

Reed, D. J. (1995). The response of coastal marshes to sea-level rise: Survival or submergence? *Earth Surface Processes and Landforms*, *20*, 39–48.

Reed, R. E., Dickey, D. A., Burkholder, J. M., Kinder, C. A., Brownie, C. (2008). Water level variations in the Neuse and Pamlico Estuaries, North Carolina due to local and remote forcing. *Estuarine, Coastal and Shelf Science*, *76*(2), 431-446.

Reimer, P. J., Bard, E., Bayliss, A., Beck, J. W., Blackwell, P. G., Ramsey, C. B., Grootes, P. M. (2013). IntCal13 and Marine13 radiocarbon age calibration curves 0–50,000 years cal BP. *Radiocarbon*, *55*(4), 1869-1887.

Reynolds-Fleming, J. V., Luettich Jr, R. A. (2004). Wind-driven lateral variability in a partially mixed estuary. *Estuarine, Coastal and Shelf Science*, *60*(3), 395-407.

Rogers, K., Wilton, K. M., Saintilan, N. (2006). Vegetation change and surface elevation dynamics in estuarine wetlands of southeast Australia. *Estuarine, Coastal and Shelf Science*, *66*(3–4), 559–569.

Saintilan, N., Williams, R. J. (2010). Short Note: The decline of saltmarsh in southeast Australia: Results of recent surveys. *Wetlands Australia, 18*, 49.

Schieder, N. W., Kirwan, M. L. (2019). Sea-level driven acceleration in coastal forest retreat. *Geology*, *47*(12), 1151–1155.

Shepard, C.C., Crain, C.M., Beck, M.W. (2011). The Protective Role of Coastal Marshes: A Systematic Review and Meta-analysis. *PLoS ONE, 6*(11), e27374.

Sousa, A. I., Lillebø, A. I., Caçador, I., Pardal, M. A. (2008). Contribution of Spartina maritima to the reduction of eutrophication in estuarine systems. *Environmental Pollution*, *156*(3), 628–635.

Stagg, C. L., Krauss, K. W., Cahoon, D. R., Cormier, N., Conner, W. H., Swarzenski, C. M. (2016). Processes Contributing to Resilience of Coastal Wetlands to Sea-Level Rise. *Ecosystems*, *19*(8), 1445–1459.

Stanturf, J. A., Goodrick, S. L., Outcalt, K. W. (2007). Disturbance and coastal forests: A strategic approach to forest management in hurricane impact zones. *Forest Ecology and Management*, *250*(1–2), 119–135.

Stuiver, M., and Reimer, P.J. (1993). Extended 14C database and revised CALIB 3.0 14C age calibration program. *Radiocarbon 35*:215–230.

Temmerman, S., Meire, P., Bouma, T.J., Herman, P.M.J., Ysebaert, T., De Vriend, H.J. (2013). Ecosystem-based coastal defense in the face of global change. *Nature, 504*(7478), 79-83.

Theuerkauf, E. J., Stephens, J. D., Ridge, J. T., Fodrie, F. J., Rodriguez, A. B. (2015). Carbon export from fringing saltmarsh shoreline erosion overwhelms carbon storage across a critical width threshold. *Estuarine, Coastal and Shelf Science*, *164*, 367–378.

Thibodeau, P. M., Gardner, L. R. Reeves, H. W. (1998).The role of groundwater flow in controlling the spatial distribution of soil salinity and rooted macrophytes in a southeastern salt marsh, USA. *Mangroves and Salt Marshes 2*, 1-13.

Thorne, K., Macdonald, G., Guntenspergen, G., Ambrose, R., Buffington, K., Dugger, B., Freeman, C., Janousek, C., Brown, L., Rosencranz, J., Holmquist, J., Smol, J., Hargan, K., Takekawa, J. (2018). U.S. Pacific coastal wetland resilience and vulnerability to sea-level rise. *Science Advances 4,* eaao3270.

Törnqvist, T.E., Gonzalez, J.L., Newsom, L., van der Borg, K., de Jong, A.F.M., Kurnik, C.W. (2004). Deciphering Holocene sea-level history on the U.S. Gulf Coast: a high-resolution record from the Mississippi Delta. *Geological Society of America Bulletin, 116*, 1026-1039.

Torio, D.D., Chmura, G.L., 2013. Assessing coastal squeeze of tidal wetlands. Journal of Coastal Research 29, 1049-1061.

United States Geological Survey Earth Explorer. (Date accessed 11/16/2018). https://earthexplorer.usgs.gov/

Van Eerden, M. R., Drent, R. H., Stahl, J., Bakker, J. P. (2005). Connecting seas: Western Palaearctic continental flyway for water birds in the perspective of changing land use and climate. *Global Change Biology*, *11*(6), 894–908.

Villarini, G., Vecchi, G.A., 2013. Projected Increases in North Atlantic Tropical Cyclone Intensity from CMIP5 Models. Journal of Climate 26, 3231-3240.

Voss, C. M., Christian, R. R., Morris, J. T. (2013). Marsh macrophyte responses to inundation anticipate impacts of sea-level rise and indicate ongoing drowning of North Carolina marshes. *Marine Biology*, *160*(1), 181–194.

Williams, K., Ewel, K.C., Stumpf, R.P., Putz, F.E., Workman, T.W. (1999). Sea-level rise and coastal forest retreat on the west coast of Florida, USA. *Ecology, 80*(6), 2045-2063.

Young, R.S. (1995). Coastal Wetland Dynamics in Response to Sea-Level Rise: Transgression and Erosion [Ph.D. dissertation]: Durham, North Carolina, Duke University, 202 p.

Zhang, Z., Colle, B.A., 2018. Impact of Dynamically Downscaling Two CMIP5 Models on the Historical and Future Changes in Winter Extratropical Cyclones along the East Coast of North America. Journal of Climate 31, 8499-8525.